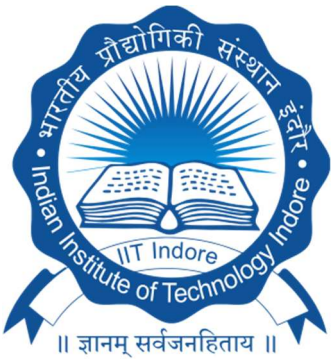
Numerical study of flow dynamics past a rounded-corner rectangular cylinder in the vicinity of a plane wall.

M.Tech. Thesis

by

POOJARY SURAJ SURESH



DEPARTMENT OF MECHANICAL ENGINEERING (ME)

INDIAN INSTITUTE OF TECHNOLOGY INDORE

MAY 2026

Numerical study of flow dynamics past a rounded-corner rectangular cylinder in the vicinity of a plane wall.

A THESIS

Submitted in partial fulfillment of the
requirements for the award of the degree
of
Master of Technology

by

POOJARY SURAJ SURESH



DEPARTMENT OF MECHANICAL ENGINEERING (ME)
INDIAN INSTITUTE OF TECHNOLOGY INDORE

MAY 2026

INDIAN INSTITUTE OF TECHNOLOGY INDORE

CANDIDATE'S DECLARATION

I hereby certify that the work which is being presented in the thesis entitled **Numerical study of flow dynamics past a rounded-corner rectangular cylinder in the vicinity of a plane wall** in the partial fulfillment of the requirements for the award of the degree of **MASTER OF TECHNOLOGY** and submitted in the **DEPARTMENT OF MECHANICAL ENGINEERING (ME), Indian Institute of Technology Indore**, is an authentic record of my own work carried out during the time period from July 2024 to May 2026 under the supervision of Prof. Dhinakaran Shanmugam, Professor, ME, Indian Institute of Technology Indore.

The matter presented in this thesis has not been submitted by me for the award of any other degree of this or any other institute.

22-05-2026
Signature of the student with date
POOJARY SURAJ SURESH

This is to certify that the above statement made by the candidate is correct to the best of my/our knowledge.

May 22, 2026
Signature of the Supervisor of M.Tech. thesis (with date)
Prof. Dhinakaran Shanmugam

POOJARY SURAJ SURESH has successfully given his/her M.Tech. Oral Examination held on **26th May 2026**.

Signature(s) of Supervisor(s) of M.Tech. thesis
Date: May 27, 2026

Convener, DPGC
Date: 27-05-2026

ACKNOWLEDGEMENTS

I would like to thank my project supervisor, Prof. Dhinakaran Shanmugam, whose guidance throughout entire course of my project has been an immense learning experience for me.

Furthermore, I would like to thank the research scholars in my CFD lab, Dheeraj Shriwas Sir, Sunil Kurrey and Arvind Patel for their time in helping me overcoming the errors and software bugs I faced during the lab session.

I would also like to thank my family members, especially my mother Mrs. Ratna Poojary, who made sure I stayed motivated throughout this M. Tech journey and also my father Mr. Suresh M. Poojary, whose unwavering support towards me helped me complete this course with utmost commitment and hard work.

I would like to convey my gratitude to my colleagues and friends at Indian Institute of Technology Indore for their help and company, which made this journey a beautiful moment filled with fun and laughter even during times of hardships.

Lastly, I am thankful to all those who indirectly contributed to this thesis and made this possible.

DEDICATION

“Dedicated to my parents for their Love, Support & Blessings.”

Abstract

Bluff bodies are characterized by flow separation, vortex shedding, wake formation and some hydrodynamic force parameters like Drag coefficient, Lift coefficient, Nusselt number, Strouhal number etc. which are usually dependent on geometric parameters and positioning of the body along its surroundings.In this current study, simulation is done on the viscous, unsteady, incompressible flow around a 2D rectangular cylinder with curved sides present close to a stationary wall in a laminar regime. The aim of this study is to give a better understanding about the effects of gap ratio along with its aspect ratio on the rectangular cylinder and flow parameters changing with it. A great influence on the wake structures forming around the body can be observed due to these two geometric parameters.

The Reynolds number is taken to be 100 based on the inflow velocity and the width of the cylinder. Simulation is carried out for three aspect ratios (A/R=1,2 & 3) and gap ratios ranging from (0.1 to 4). Conditions are taken such that it helps in clearly observing the vortex shedding behaviour and a detailed analysis of wake formation can be done. Flow visualization parameters like vorticity distribution, streamlines, pressure fields and hydrodynamic forces like Strouhal number, Drag and Lift coefficient are calculated and presented in this paper. Influence of the stationary plate adjacent to the cylinder can be seen on the wake formation behind the cylinder. Also, alteration in the separation process can be seen for the bluff body considered although for higher gap ratios, a resemblance with isolated case can be seen.

The parameters studied provide a quantitative nature of the flow behaviour. With change in aspect ratios, a change in geometry of the bluff body is aimed to achieve. Which in return also influences the flow just like change in gap ratios.

TABLE OF CONTENTS

LIST OF FIGURES IX

LIST OF TABLES XII

NOMENCLATURE XIII

Chapter 1: Introduction 1

1.1 Background 1

1.2 Bluff body 2

1.3 Drag 3

1.4 lift 3

1.5 CFD Simulations 5

1.5.1 Pre-processing 6

1.5.2 Solving 6

1.5.3 Post processing 7

1.6 Summary and dissertation 7

Chapter 2: Literature review and Problem Formulation 9

2.1 Literature survey 9

2.2 Research gap 11

2.3 Objective of this work 12

2.3.1 Aspect ratio, its influence 12

2.3.2 Gap ratio, its influence 13

Chapter 3: Methodology 15
3.1 Grid dependency test 15
3.2 Model validation 17
3.2.1 Circular cylinder simulation 17
3.2.2 Rectangular cylinder simulation 19
3.3 Governing equations and computational methods 21
3.4 Boundary conditions 22
Chapter 4: Results and discussions 24
4.1 Flow characteristics 24
4.1.1 Time evolution of lift coefficient and drag coefficient 24
4.1.2 Instantaneous vorticity pattern 28
4.1.3 Vortex shedding during a cycle at different G/D. 28
4.1.4 Time averaged streamlines 32
4.1.5 Time averaged velocity streamline for Aspect ratio A/R=3,2 & 1 at different G/D. 33
4.1.6 Pressure coefficient contour for Aspect ratio A/R=3,2 & 1 at different G/D. 38
4.1.7 Isotherms for Aspect ratio A/R=3,2 & 1 during a cycle at different G/D. 44
4.2 Drag coefficients 50
4.2.1 Time averaged Drag coefficient 50
4.3 Lift coefficients 51
4.3.1 Time averaged lift coefficients 52
4.4 Pressure coefficient 53

4.4.1 Distribution of time averaged pressure coefficient on the surface of the square cylinder for A/R=1,2 &3. 53
4.4.2 Average Pressure coefficient (Cp) along the faces of rectangular cylinders for A/R=1,2 & 3. 55
4.4.3 Mean Pressure coefficient 57
4.5 Strouhal number 58
4.6 Recirculation length 60
4.7 Nusselt number 61
4.7.1 Distribution of time average local Nusselt number along the surface of the rectangular cylinder for A/R=1,2 & 3. 61
4.7.2 Average Nusselt number along the faces of rectangular cylinder for A/R=1,2 & 3. 63
4.7.3 Mean Nusselt number 65
Chapter 5: Summary and Conclusions 67
REFERENCES 69

LIST OF FIGURES

Fig. 1 Schematic representation of streamline body and bluff body.

Fig. 2 Schematic representation of drag and lift force acting on an aeroplane.

Fig. 3 Flow chart showcasing different stages in CFD numerical simulation.

Fig. 4 Schematic representation of bluff bodies of aspect ratio 1,2 & 3.

Fig. 5 Schematic representation of bluff bodies of gap ratio 4,1 & 0.3.

Fig. 6 Schematic representation of non-uniform meshing used for A/R 2 & 3 in vicinity to a stationary wall.

Fig. 7 Sketch of the flow configuration for the uniform flow past a heated circular cylinder.

Fig. 8 Schematic representation of non-uniform meshing used for circular cylinder.

Fig. 9 Time evolution of drag coefficient (C_D, orange line) and lift coefficient (C_l, blue line) at Re=100, for the flow past a circular cylinder.

Fig. 10 Pressure coefficient contour for flow past a circular cylinder.

Fig. 11 Instantaneous vorticity contour for flow past a circular cylinder.

Fig. 12 Sketch of the flow configuration for the uniform flow past a heated rectangular cylinder with rounded corners present between two solid wall boundaries.

Fig. 13 Comparison of present study (blue line) and results of R. Wang et. al. for variation of Drag Coefficient C_D at different aspect ratios A/R for the uniform flow past a heated rectangular cylinder with rounded corners present between two solid wall boundaries.

Fig. 14 Comparison of present study (blue line) and results of R. Wang et. al. for variation of Strouhal number St at different aspect ratios A/R for the uniform flow past a heated rectangular cylinder with rounded corners present between two solid wall boundaries.

Fig. 15a Instantaneous vorticity contour for rectangular cylinder with aspect ratio A/R=1 at different gap ratios.

Fig. 15b Time evolution of lift coefficient and drag coefficient for rectangular cylinder with aspect ratio A/R=1 at different gap ratios.

Fig. 16 Instantaneous vorticity contour for rectangular cylinder with aspect ratio A/R=1,2 & 3

Fig. 17 Instantaneous vorticity contour for rectangular cylinder with aspect ratio A/R=2 & 3 with respect to different gap ratios.

Fig. 18 Time averaged streamlines for different aspect ratios.

Fig. 19 Time averaged velocity streamline for Aspect ratio A/R=3,2 & 1 at different G/D.

Fig. 20 Pressure coefficient contour for Aspect ratio A/R=3,2 & 1 at different G/D.

Fig. 21 Isotherms for Aspect ratio A/R=3,2 & 1 during a cycle at different G/D.

Fig. 22 Variation of mean Drag coefficient C_D vs gap ratio for different aspect ratio of A/R = 1,2 & 3.

Fig. 23 Variation of mean Lift coefficient C_l vs gap ratio for different aspect ratio of A/R = 1,2 & 3.

Fig. 24 Distribution of time averaged pressure coefficient C_p on the surface of the body of aspect ratio A/R=3 near a stationary wall as a function of gap ratio, G/D.

Fig. 25 Distribution of time averaged pressure coefficient C_p on the surface of the body of aspect ratio A/R=2 near a stationary wall as a function of gap ratio, G/D.

Fig. 26 Distribution of time averaged pressure coefficient C_p on the surface of the body of aspect ratio A/R=1 near a stationary wall as a function of gap ratio, G/D.

Fig. 27 Average Pressure coefficient (C_p) along the faces of rectangular cylinders for A/R=3 at different gap ratios G/D.

Fig. 28 Average Pressure coefficient (C_p) along the faces of rectangular cylinders for A/R=2 at different gap ratios G/D.

Fig. 29 Average Pressure coefficient (C_p) along the faces of rectangular cylinders for A/R=1 at different gap ratios G/D.

Fig. 30 Variation of mean Pressure coefficient C_p vs gap ratio for different aspect ratio of A/R = 1,2 & 3.

Fig. 31 Variation of Strouhal number St vs gap ratio for aspect ratio of A/R = 1.

Fig. 32 Variation of Recirculation length L vs gap ratio for different aspect ratio of A/R = 1,2 & 3.

Fig. 33 Distribution of time averaged Nusselt number Nu on the surface of the body of aspect ratio A/R=3 near a stationary wall as a function of gap ratio, G/D.

Fig. 34 Distribution of time averaged Nusselt number Nu on the surface of the body of aspect ratio A/R=2 near a stationary wall as a function of gap ratio, G/D.

Fig. 35 Distribution of time averaged Nusselt number Nu on the surface of the body of aspect ratio A/R=1 near a stationary wall as a function of gap ratio, G/D.

Fig. 36 Average Nusselt number Nu along the faces of rectangular cylinders for A/R=3 at different gap ratios G/D.

Fig. 37 Average Nusselt number Nu along the faces of rectangular cylinders for A/R=2 at different gap ratios G/D.

Fig. 38 Average Nusselt number Nu along the faces of rectangular cylinders for A/R=1 at different gap ratios G/D.

Fig. 39 Variation of mean Nusselt number Nu vs gap ratio for different aspect ratio of A/R = 1,2 & 3.

LIST OF TABLES

Table 1 Results of grid dependency test comparing present data with results of V. Eswaran et al [4] for avg. Nusselt number Nu.

Table 2 Results of grid dependency test comparing present data with results of V. Eswaran et al [4] for avg. Drag coefficient C_D.

Table 3 Validation results for flow around circular cylinder.

NOMENCLATURE

AB	Front face of the cylinder
BC	Bottom face of the cylinder
CD	Rear face of the cylinder
DA	Top face of the cylinder
D	Height of the rectangular cylinder
C_l	Lift coefficient,
C_D	Drag coefficient,
C_p	Pressure coefficient,
f	Frequency of vortex shedding,
G	Dimensional distance between the bottom surface of cylinder and the plane wall
G/D	Gap ratio or non-dimensional distance between the bottom surface of cylinder and the plane wall
k	Thermal conductivity
L_{us}	Length of upstream boundary from the front face of the cylinder
L_{ds}	Length of downstream boundary from the rear face of the cylinder
L_h	Length of top boundary from the top face of the cylinder
Nu	Nusselt number of the cylinder,
Pr	Prandtl number,
Re	Reynolds number,
St	Strouhal number,

t Dimensional time

F_D Drag force,

A Reference area,

ρ Density of fluid,

U_∞ Free stream velocity,

A/R Aspect ratio of the rectangular cylinder,

D Characteristic length,

u Horizontal component of velocity,

v Vertical component of velocity,

μ Dynamic viscosity,

Chapter 1 Introduction

1.1 Background

One of the central problems in fluid mechanics, as observed in real life applications, is the flow past non-streamlined geometry also known as bluff body. Occurrence of unsteady wake formation with generation of vortices due to separation of boundary layer can be seen as soon as the flowing fluid encounters the bluff body. One of the important parameters being the drag force acting on the body which in return influences the performance and stability of the body. Objects with sharp corners and much bigger frontal areas tend to have dominant pressure components as seen in many applications.

Square cylinder is one of the bluff body geometries which have received considerable attention due to their applications in architectural design, bridge building, electronic devices, and ship building. Due to presence of edges of the bluff body geometry, there will be early flow separation leading to formation of a large wake region. Hence, the square cylinder has become an excellent geometry for investigations in flow control and drag reduction in aerodynamic research.

It is very important to improve the aerodynamic performance of these bluff body geometries so that there can be a reduction in the external forces acting on these systems and increase the life span. Several passive and active methods have been suggested for managing the separated flow over bluff body geometries.

Nonetheless, passively managed flows enjoy tremendous preference owing to the non-reliance on energy input from external sources. Cut-corner approach is one of those passive approaches that involve cutting the sharp edges of a square cylinder to affect the behavior of the flow around the body. The effects of corner cutting may include reduced wake development, alter vortex shedding, and less drag force acting on the body. While this approach has shown promising outcomes, its impact on the flow and drag reduction remains an interesting subject of research. In this context, this research focuses on employing the cut-corner approach in achieving improved drag reduction characteristics of a square cylinder.

1.2 Bluff body

Bluff bodies are bodies with non-streamlined shapes that disturb the flow and create separation, wake formation, and strong pressure drag. They are widely studied in fluid mechanics because their flow behavior is highly unsteady and strongly influenced by geometry, Reynolds number, and boundary-layer separation.

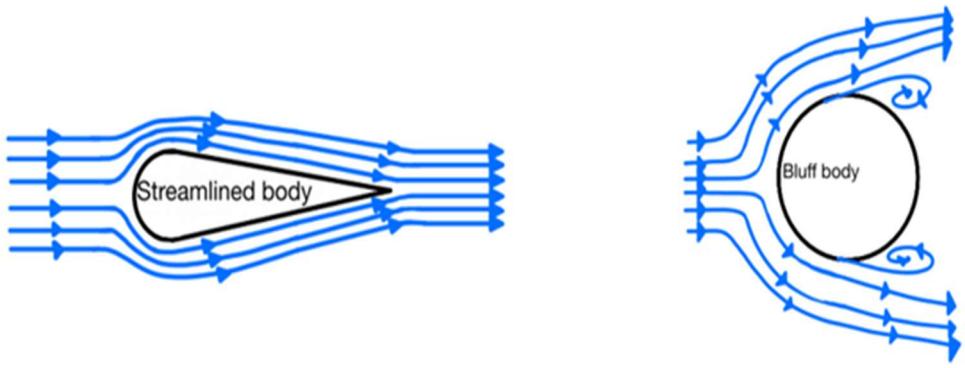


Fig. 1. Schematic representation of streamline body and bluff body.

Bluff bodies in the form of square cylinders represent some of the bluff body shapes that have gained great attention owing to their use in architectural applications, bridge design, electronics, and naval engineering. The sharp edges of the bluff body shape create early flow separation, creating a large wake region and causing a pressure drop. In effect, the square cylinder is seen as the perfect bluff body shape for investigating flow control and drag reduction in aerodynamic research. Enhancing the aerodynamic properties of these shapes is essential in decreasing the external force acting on engineering systems and prolonging their lifespan.

There are a number of suggested techniques both active and passive for regulating the flow separation process of bluff body shapes. Passive flow control methods are very popular due to the absence of additional energy requirements and ease of implementation. In the perspective of CFD, the flow around the bluff body is significant since it enables scientists to determine the characteristics of pressure, drag coefficient, flow wake, and heat transfer under varying flow conditions. The application of CFD in the engineering sector is usually employed to investigate various changes on geometry, including corner rounding and chamfering.

1.3 Drag

Drag is the force that opposes the motion of a body moving through a fluid, such as air or water. The drag coefficient is a dimensionless number that tells how much drag a body experiences compared with the fluid density, flow speed, and reference area. For a body moving in a fluid, drag force is commonly written as

$$F_d = \frac{1}{2}\rho U^2 C_d A,$$

where F_d is drag force, ρ is fluid density, U is relative velocity, C_d is drag coefficient and A is the reference area.

A higher drag coefficient means the body faces more resistance, while a lower value means smoother flow and less resistance. In bluff bodies, drag is usually high because the flow separates early, creating a large wake and strong pressure difference between the front and rear surfaces. That is why bluff bodies generally have much larger drag coefficients than streamlined bodies.

1.4 Lift

Lift is the force that acts perpendicular to the direction of flow, while the lift coefficient is a dimensionless number that measures how effectively a body generates lift relative to fluid density, speed, and reference area. The lift force is commonly written as,

$$L = \frac{1}{2}\rho V^2 A C_L,$$

where L is lift, ρ is fluid density, V is flow velocity, A is reference area, and C_L is the lift coefficient.

A higher lift coefficient means the body produces more lift for the same flow conditions.

In aerodynamics, lift coefficient depends on shape, angle of attack, Reynolds number, and flow conditions. It is especially important for air foils, wings, and other lifting bodies because it helps compare performance across different designs.

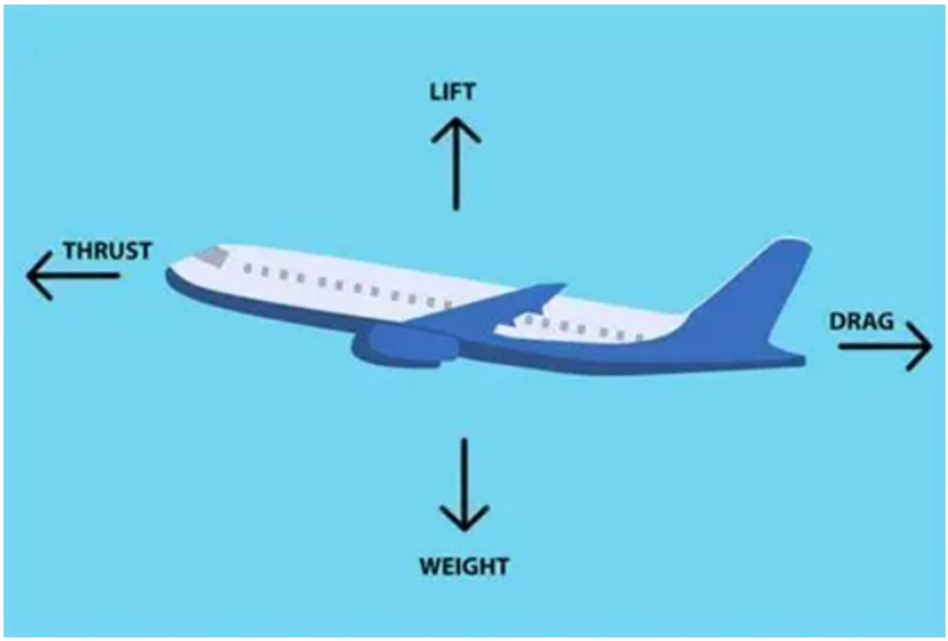


Fig. 2. Schematic representation of drag and lift force acting on an aeroplane.

The coefficients of drag and lift play the key role of being the basic quantitative parameters in any simulations related to bluff bodies in flow environment. These coefficients are basically the cumulative effect of pressure distribution and wall friction along the body's surface, making their computation necessary from the point of view of characterizing the interaction between the fluids and solids. In the engineering domain, drag defines the resistive force along the direction of the flow. Drag plays an important role in the design and construction of vehicles, offshore pipelines, heat exchangers, and wind/water-exposed structures, among other things. Lift, however, refers to the transverse force component orthogonal to the direction of flow, and predicting it accurately plays a critical role in cases such as bridge deck aerodynamics, wind turbine blades, marine risers, and subsea structures where an unchecked transverse loading can cause structural fatigue and eventual failure. In the case of near-wall bluff body flows, the drag and lift forces play an even more interesting and crucial role. In the small gap regimes, the Venturi effect creates a low-pressure zone resulting in negative lift forces pushing the body against the wall. With increasing gap ratios, the suction effect becomes less effective, and lift begins to become positive, indicating a transition in the nature of the flow.

1.5 CFD Simulations

Computational Fluid Dynamics, or CFD, is the use of numerical methods and computer-based models to study fluid flow, pressure, temperature, and related physical phenomena in engineering systems. It is widely used to predict how fluids behave around objects before building or testing the actual system.

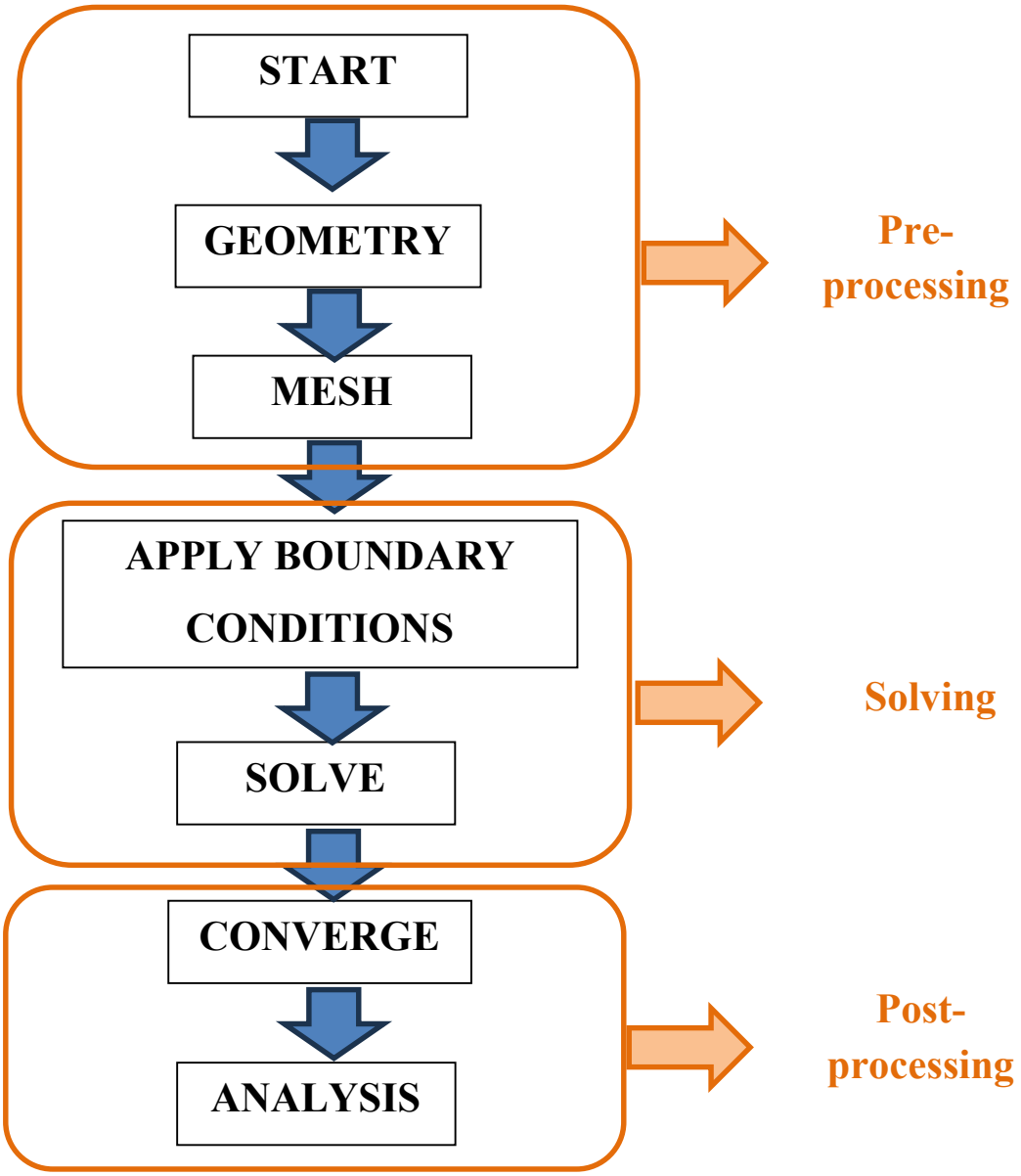


Fig. 3. Flow chart showcasing different stages in CFD numerical simulation.

A CFD simulation usually follows a standard workflow: define the geometry, create a mesh, apply boundary and initial conditions, solve the governing equations, and then post-process the results. The governing equations are based on fluid mechanics principles such as the Navier-Stokes equations, which describe the motion of fluids.

CFD is especially useful in analyzing bluff body flows, where flow separation, wake formation, and vortex shedding make the problem difficult to solve analytically. By using CFD, engineers can evaluate drag, pressure distribution, heat transfer, and flow-induced vibration around different body shapes and design conditions.

In simple terms, CFD simulations help engineers test ideas virtually, reduce experimental cost, and improve design performance in areas like aerodynamics, thermal management, turbomachinery, and electronic cooling.

1.5.1 Pre-processing

Introduction of the CFD quality problem is a major part of the pre-processing part. This includes preparation for the problem for computation. Some of the key tasks include creating the geometry, definition of the domain, generation of mesh, material setup, providing initial and boundary conditions and completed by setting up the solver.

Geometry being the important part of the pre-processing part as it has direct effects on the mesh quality and solver stability for the computational problem.

Following by mesh generation, which is a central part, where the entire domain is converted into refined and discrete cells for study of gradients, wakes and separation zones occurring in the different regions of the domain. The common methodology for mesh generation includes a coarse to fine mesh structure for achieving greater sensitivity at a particular desired region.

1.5.2 Solving

In the solving stage, the governing equations are converted into discrete algebraic equations using numerical methods such as the finite volume method. These equations are usually solved iteratively, so convergence checking is a major part of this stage. For transient simulations, the

solver also advances the solution in time, while steady simulations seek a time-independent final state.

CFD uses numerical methods because analytical solutions exist only for very simple flows and geometries. The solver choice depends on the physics: incompressible, compressible, laminar, turbulent, steady, or transient. Iterative convergence and stability are key indicators of whether the solution is trustworthy

1.5.3 Post processing

Post-processing is where you extract meaning from the computed flow field. Common outputs include contour plots, streamlines, vectors, surface plots, and integrated quantities such as lift, drag, pressure drop, or thrust. Tools like ParaView and Tecplot are widely used for visualization and quantitative analysis of CFD results.

Post-processing is not only visualization; it also includes data extraction and validation. Comparing CFD results with analytical, computational, or experimental data is important for credibility.

For unsteady flows, post-processing may include identifying statistical steady state and averaging overtime windows.

1.6 Summary and dissertation

Current thesis aims to analyse and find out the optimum gap ratio G/D and Aspect ratio A/R for desired flow parameters and hydrodynamics forces of rectangular bluff body with rounded corners in vicinity to a stationary plane wall when placed in presence of a flow. As aspect ratio increases there is a geometric variation along lengthwise of the body which have certain effects on the flow around the body. Similarly with decreasing gap ratios also lead to certain changes in the hydrodynamic flow past the body.

For this thesis investigation, computational fluid dynamics CFD simulations in ANSYS Fluent is used and flow characteristics for laminar flow regime with Re==100 is studied.

From the results of the simulations and analysing it, therefore, for higher gap ratios like G/D =4, where influence of the adjacent stationary wall is negligible a reduction of 4.8% can be seen as we move up from aspect ratio A/R of 2 to 3. Although the difference diminishes when body is brought closer to the stationary wall. Similarly, there is a decrease of 15.20 % in heat transfer with increase in aspect ratio A/R of 2 to 3 considering for highest gap ratio G/D=4 at Re=100.

Hence, it can be said that variation in geometric aspects of the body can alter the aerodynamic flow parameters providing desired advantages for real life applications.

Chapter 2 describes similar studies, describing about flow around bluff bodies and the nature of flow parameters following them. It mainly focuses on study showcasing effects of plane wall adjacent to the body and changes observed when it is brought closer at different instances.

Chapter 3 explains the methodology applied in this thesis starting from considering accurate grid model for the selected domain. Followed by model validation for various geometries and flow conditions. Also showcasing the governing equations used for said calculation.

Chapter 4 represents the results achieved in this study in detailed manner and comparisons played out for different aspect ratios and gap ratios.

Chapter 5 finalizes the thesis with proper conclusions found and gives a summary of the study done.

Chapter 2

Literature Review and Problem formulation

The motive of this chapter is to display previous studies done on similar bluff bodies which showcases the effects of gap ratios and aspect ratios on the flow around the body. Also finding out the research gap in the studies for current and future scope on related problems similar to the one done during this project.

2.1 Literature survey

Previously, numerical simulation on similar shape can be seen done (R. Wang et al. 2024)[1] where the impact of Reynold number (Re), Aspect ratio and rounded corners on the flow parameters were studied and in (J.Zhou 2024)[2] where a comprehensive study was done on semi submerged rectangular cylinder with rounded corners and its impact on the hydrodynamic characteristics.

There is another research work (Zhai et al 2022)[3] conducted on the Effect of the Gap Ratio on the flow and heat transfer over a bluff body in near-wall conditions. In this research, the impact of varying gap ratios on the thermofluidic domain of a bluff body in proximity to a heated surface was evaluated using experimental and numerical techniques. According to the findings, gap ratio acts as an important parameter which influences wake dynamics – specifically, for low gap ratios, the effect is significant.

In a study examining the effects of the Gap Ratio on the coherent structures formed around a near-wall square cylinder carried out by (H. Chalmers et al 2022)[4], there is also analysis on the turbulence separation created by sharp-edged bluff bodies that are held in close proximity to a rough wall, in applications such as raised pathways, trucks, and heat exchangers, which shows that the critical gap ratio where vortex shedding ceases lies between 0.2 to 0.5.

In addition, another study conducted by (Helmizar et al 2025)[5] entitled "Flow Characteristics Around Circular and Rectangular Bluff Bodies in the Vicinity of a Wall for Various Gap Ratios," compares the flow behavior of the bluff body with circular and rectangular sections of various gap

ratios that range from G/D = 0.065 to 2.0. For G/D=0.065, the interaction will be at its maximum between the bluff body and the wall, which will cause the deflection of the flow and hence the creation of the wake flow.

The research carried out by (M. Shineeb 2018)[6], which examined the effect of gap flow on the wake of a sharp-edged bluff body – Coherent structures, explored the characteristics of turbulent wake formed due to a vertical flat plate placed in a shallow channel where there is a gap near the bed. Some of the main discoveries made by the researcher include the creation of three-dimensional hairpin like vortex loop just after the bluff body, with gap flow decreasing vortex loop diameter and increasing spinning.

Two-Dimensional vortex shedding from a circular cylinder adjacent to a moving wall this research, done by (Bearman and Zdarkovich 2006)[7], uses numerical simulation of a flow over a circular cylinder adjacent to a moving wall to develop a quantitive measure for the determination of vortex shedding suppression point. Suppression of vortex shedding is achieved with a gap ratio of 0.2-0.3 depending on the boundary layer thickness. As the thickness of the boundary layer increases, the gap ratio decreases.

The effects of rounded corners on a rectangular body is shown in (E. Lamballais 2010)[8] where influence of curvature of square cylinder on fluid flow is investigated and its impact is studied. (T. Abdelhamid et al. 2021)[9] studied the effects of corner radius ranging from 0 to 1 turning the square cylinder into a circular one along with its changing attack angle. The study was carried out for Re varying from 40 to 150 where the variation of flow patterns, aerodynamic forces were analysed.

Similarly, the effect of a moving plane wall placed adjacent to a square bluff body (S. Dhinakaran 2011)[10] where it shows the variation of parameters such as lift and drag coefficients, Strouhal number, pressure distribution and Nusselt number of the cylinder with different gap ratios. This study successfully describes that a plane wall present adjacent to a bluff body has great influence on the flow parameters surrounding the body. Another such study focussing on the effects of gap ratios around square cylinders is done by (S. Tanweer et. al. 2018)[11] where a constant Re=30 is considered and the effects on the flow parameters are considered.

2.2 Research gap

From all the works mentioned above, the main focus of the studies can be seen to be around the shape dependency on the flow parameters and there might not be seen presence of any stationary wall beside the particular shape of the body and its effects on the body. Some of the studies like (Zhai et al 2022)[3], (H. Chalmers et al 2022)[4], (Helmizar et al 2025)[5] do study about gap ratios but it is focused mainly on bluff bodies with sharp edge geometries. On the contrary studies like Lamballais (2010)[8] and Abdelhamid et al. (2021)[9] have considered rounded corners but there is no presence of any wall in proximity nor any consideration of gap ratios.

One such study which focuses on rounded corners is Zhou (2024)[2], but effects produced by varying the gap ratio is not investigated here. Study by Zhai et al. (2022)[3] investigated flow analysis and heat transfer around a generic bluff body with no corner rounding presence, hence, there is no study focusing on thermal analysis around bluff body with rounded cornered geometry considering a varying gap ratio with an plane wall present in proximity.In Zhou's (2024)[2] investigation of the effects of semi-submerged rounded rectangular structures, study on some hydrodynamic features were involved, however, gap ratio was not considered as an important parameter to control. Also, in the analysis of gap flow in shallow channels, Shinneeb (2018)[6] used a sharp-flat plate only; therefore, a semi-submerged rounded rectangular body at different gap ratios has yet to be studied. There is evident study for Chalmers et al.'s (2022)[4] and Bearman and Zdravkovich's (2006)[7] investigations of critical gap ratios that lie between 0.2 to 0.5; however, these studies were carried out on limited gap ratios. This means that the critical gap ratio for suppression of vortex shedding in a rounded bluff body can hardly be defined due to the fundamental differences.The effect of aspect ratio for a rounded rectangular body was studied by Wang et al. (2024)[1], and Helmizar et al. (2025)[5] examined the effects of gap ratio; nevertheless, the relationship between aspect ratio and gap ratio has never been addressed in a rounded rectangular body.

Therefore, it can be said that there is a need to study the how rounded corner of different aspect ratios and gap ratio interact with the flow parameters around the bluff body.

Current study focuses on the effects of a stationary plane wall present adjacent to the body of three different aspect ratios A/R=1,2 & 3, on the flow parameters and hydrodynamic forces, as the body is brought closer to the wall at different gap ratios ranging from 0.1 to 4.

2.3 Objective of this work

2.3.1 Aspect ratio, its influence

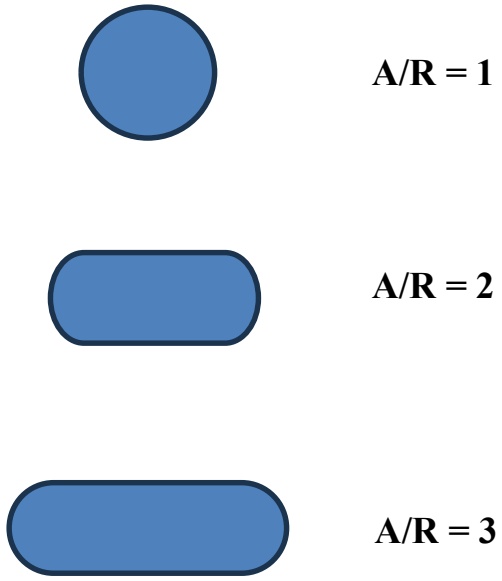


Fig. 4. Schematic representation of bluff bodies of aspect ratio 1,2 & 3.

Above figure shows the geometric representation of a body at three different ratios i.e. at A/R=1,2 & 3 (from top to bottom respectively). It can be seen that as the aspect ratio increases there is a lengthening of the body along the x-direction. Aspect ratio is a key geometric parameter that strongly influences the flow around a bluff body in laminar regime. It affects the separation point, wake size, recirculation zone, pressure distribution, and vortex shedding behavior. For lower aspect ratios, the flow often separates earlier and creates a wider wake with stronger pressure drag, while higher aspect ratios may delay separation and modify the wake structure. The aspect ratio also changes the vortex shedding frequency, which influences the Strouhal number and unsteady lift fluctuations. Since laminar flow is highly sensitive to geometry, even small changes in aspect ratio can produce noticeable differences in flow behavior. Therefore, accurate mesh refinement near the surface and in the wake region is essential to capture these effects properly in CFD.

2.3.2 Gap ratio, its influence

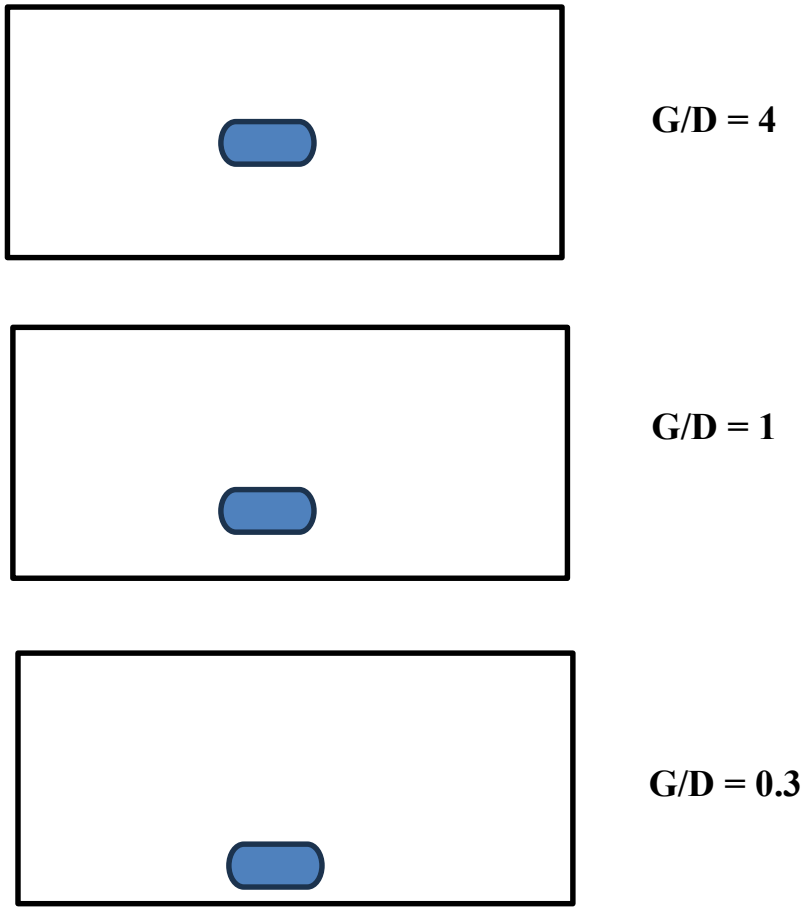


Fig. 5. Schematic representation of bluff bodies of gap ratio 4,1 & 0.3.

Above figure represents the orientation of the rectangular body with its computational domain when placed at three different gap ratios G/D= 4,1 & 0.3 (from top to bottom respectively) with respect to plane stationary wall at the bottom. With decreasing gap ratios, the body comes closer to the stationary wall which causes in formation of a much narrower gap between the body and the wall resulting in obstruction of the flow flowing below the body. Gap ratio is an important geometric parameter in laminar bluff-body flow because it strongly influences the flow structure near the wall. As the gap between the bluff body and the wall changes, the separation pattern, wake shape, pressure distribution, drag coefficient, and vortex shedding behavior also change. A small gap can accelerate the flow through the narrow passage and create a distorted wake, while a larger gap may allow a more developed and symmetric flow field. Therefore, accurate CFD analysis of

gap ratio effects requires fine mesh resolution in the gap and wake regions to capture the strong velocity and pressure gradients

Chapter 3

Methodology

3.1 Grid dependency test

A non-uniform grid distribution is used for following model simulation. Below figure describes the structure of the meshing used. It can be observed that the mesh becomes finer and finer as it comes close to the bluff body compared to the coarse mesh that are away from the body.

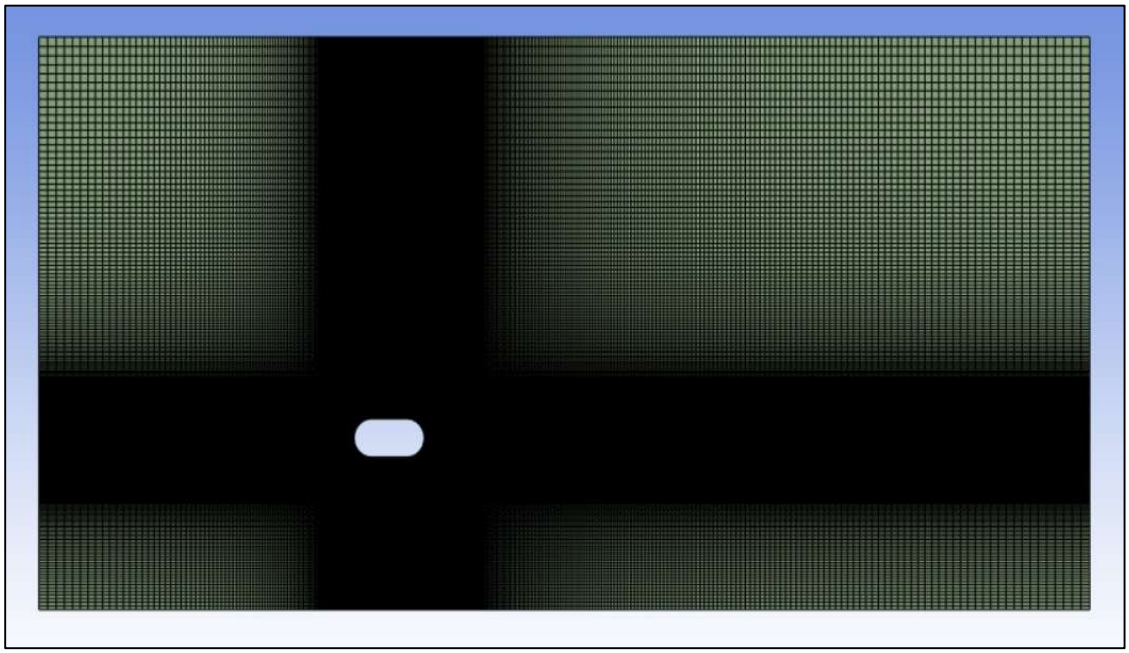


Fig. 6. Schematic representation of non-uniform meshing used for A/R 2 & 3 in vicinity to a stationary wall.

A progressive grid dependency test are performed to test and validate the following mesh for further calculations. Five types of grid sizes are employed for this grid dependency test denoted as Grid A, Grid B, Grid C, Grid D & Grid E. The test was performed referring to study on heat and fluid flow analysis on a square cylinder present in a 2d flow regime by Atul Sharma and V. Eswaran [4]. The results of the following test are mentioned below Table 1 and Table 2.

Table 1. Results of grid dependency test comparing present data with results of V. Eswaran et al [4] for avg. Nusselt number Nu.

Grid	Avg. Nusselt number (present value)	Avg. Nusselt number (from research paper)	Error%
Grid A	3.7729	4.0539	6.931
Grid B	3.9917	4.0539	1.534
Grid C	4.0294	4.0539	0.604
Grid D	4.0265	4.0539	0.675
Grid E	4.0244	4.0539	0.727

Table 2. Results of grid dependency test comparing present data with results of V. Eswaran et al [4] for avg. Drag coefficient CD.

Grid	Avg. Drag coefficient (present value)	Avg. Drag coefficient (from research paper)	Error%
Grid A	1.7269	1.494	15.589
Grid B	1.6073	1.494	7.583
Grid C	1.5136	1.494	1.311
Grid D	1.5064	1.494	0.829
Grid E	1.5018	1.494	0.522

From the above data it is clear that Grid E posses the least percentage error for the recorded parameters, hence Grid E can be finalized for further simulations.

Since our bluff body is a rectangular bluff body with rounded edges, a numerical study of effects of aspect ratio on rectangular cylinder [R. Wang et. al][1] resembles similar geometry to current study. A validation of the said study under selected grid size is carried out and their Comparison of the results is shown in below Fig 2 and Fig 3.

3.2 Model Validation

3.2.1 Circular cylinder simulation

A classical bluff body problem in the domain of CFD is the study of flow around a circular cylinder to learn about the wake formation, drag, lift and vortex shedding around the body. Similar study is done by S. Moghaddam et al. 2011[12] and a simulation for validating the study is carried out whose results are shared below. The behaviour of the flow can be seen to be strongly dependent on the Reynolds number i.e. a steady and symmetric flow can be observed for low Reynolds number whereas the flow turns out to be unsteady and periodic as the Reynolds number increases.

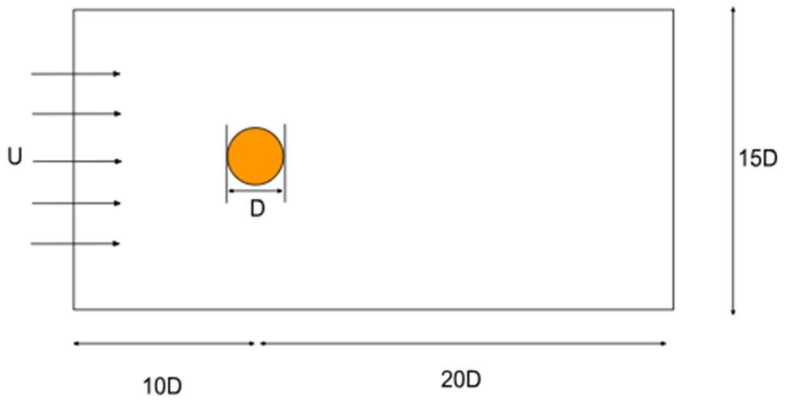


Fig. 7. Sketch of the flow configuration for the uniform flow past a heated circular cylinder.

Above figure shows the computational domain for the simulation carried for flow around circular body, a circular body of diameter D is placed in domain of size 30D X 15D with fluid flowing with inlet velocity U in x direction. The upstream length and downstream length from the cylinder

being 9.5D and 19.5D respectively. A no slip condition is considered for the top and bottom boundary with pressure outlet at the exit.

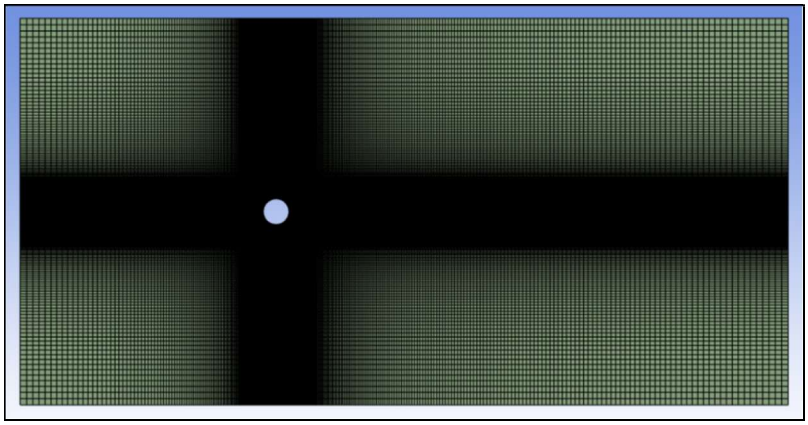


Fig. 8. Schematic representation of non-uniform meshing used for circular cylinder.

A non-uniform mesh is created for the simulation as displayed in the above figure, transitioning from finer mesh at the region closer to the body to much more coarser mesh at the boundary of the domain.

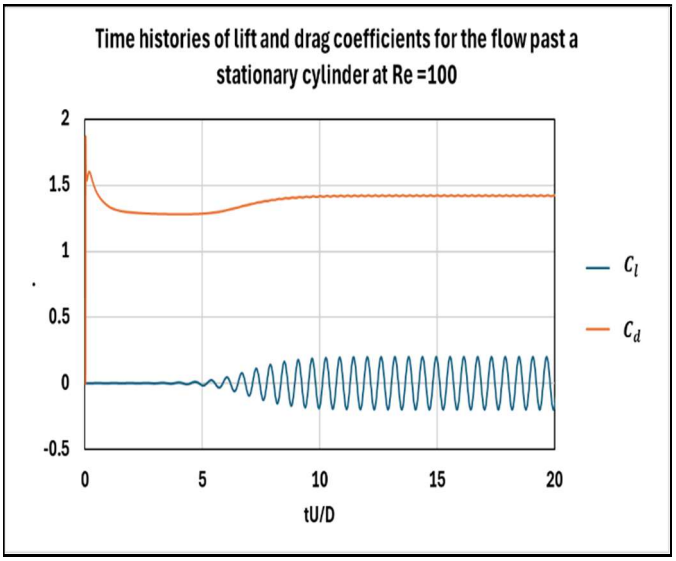


Fig. 9. Time evolution of drag coefficient (CD, orange line) and lift coefficient (Cl, blue line) at Re=100, for the flow past a circular cylinder.

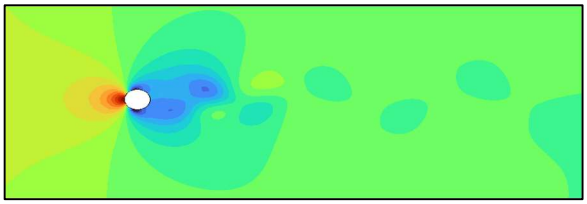


Fig. 10. Pressure coefficient contour for flow past a circular cylinder.

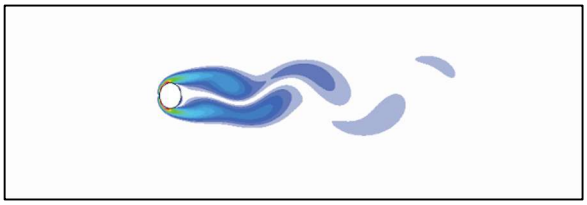


Fig. 11. Instantaneous vorticity contour for flow past a circular cylinder.

Table 3. Validation results for flow around circular cylinder.

	Exp results	Numerical results				
	S. Kang [13]	Liu et al. [14]	Lee and Yang [15]	Park et al. [16]	S. Moghaddam et al. [12]	Present work
Cd	1.33	1.37	1.34	1.33	1.36	1.35
Cl	0.32	0.33	0.33	0.33	0.36	0.000764
St	0.165	0.165	0.165	0.165	0.166	0.162

Above Table shows a comparison of mean drag coefficient (Cd), mean lift coefficient (Cl) and Strouhal number (St) , for a single cylinder at Re =100.

3.2.2 Rectangular cylinder simulation

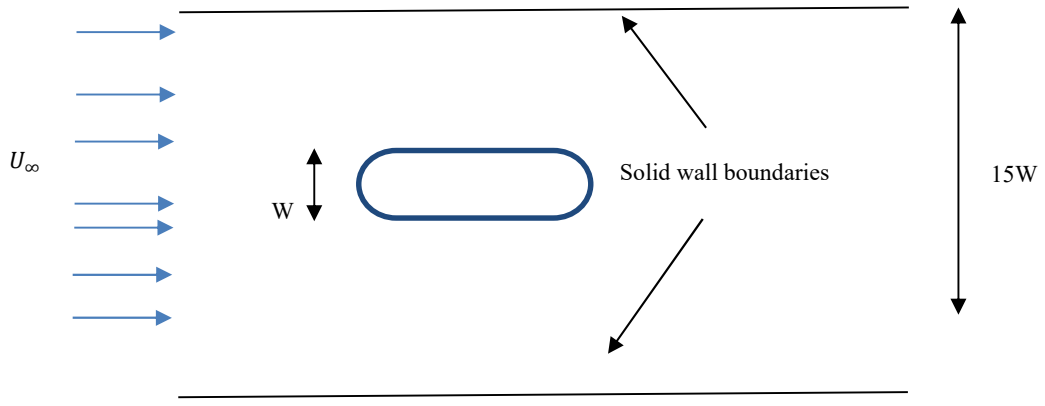


Fig. 12. Sketch of the flow configuration for the uniform flow past a heated rectangular cylinder with rounded corners present between two solid wall boundaries.

Pier sections for high-speed railways normally have a rectangular-like cylindrical form with rounded corners. This design is quite common; to study the variation of the fluid characteristics for rectangular-like, rectangular, and square cross-sections, it was decided to use a physical model of high-speed railway bridges piers is simplified as a rectangular-like cylinder with rounded corners, which is studies in R. Wang et. al. [1]

Since our bluff body is a rectangular bluff body with rounded edges, a numerical study of effects of aspect ratio on rectangular cylinder [R. Wang et. al][1] resembles similar geometry to current study. A validation of the said study under selected grid size is carried out and their Comparison of the results is shown in below Fig 2 and Fig 3.

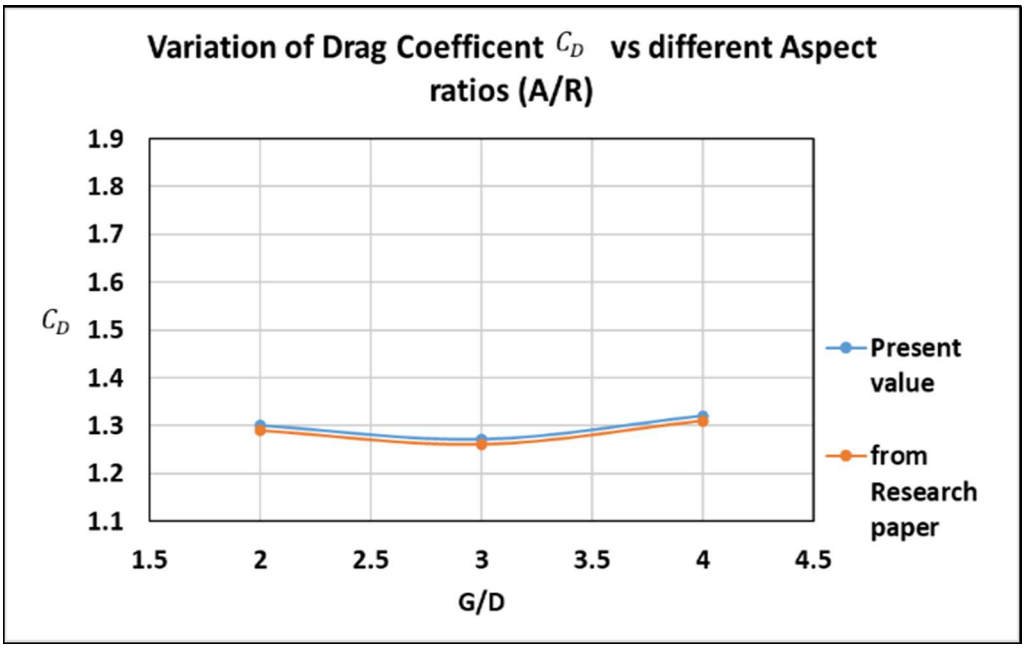


Fig. 13. Comparison of present study (blue line) and results of R. Wang et. al. for variation of Drag Coefficient CD at different aspect ratios A/R for the uniform flow past a heated rectangular cylinder with rounded corners present between two solid wall boundaries.

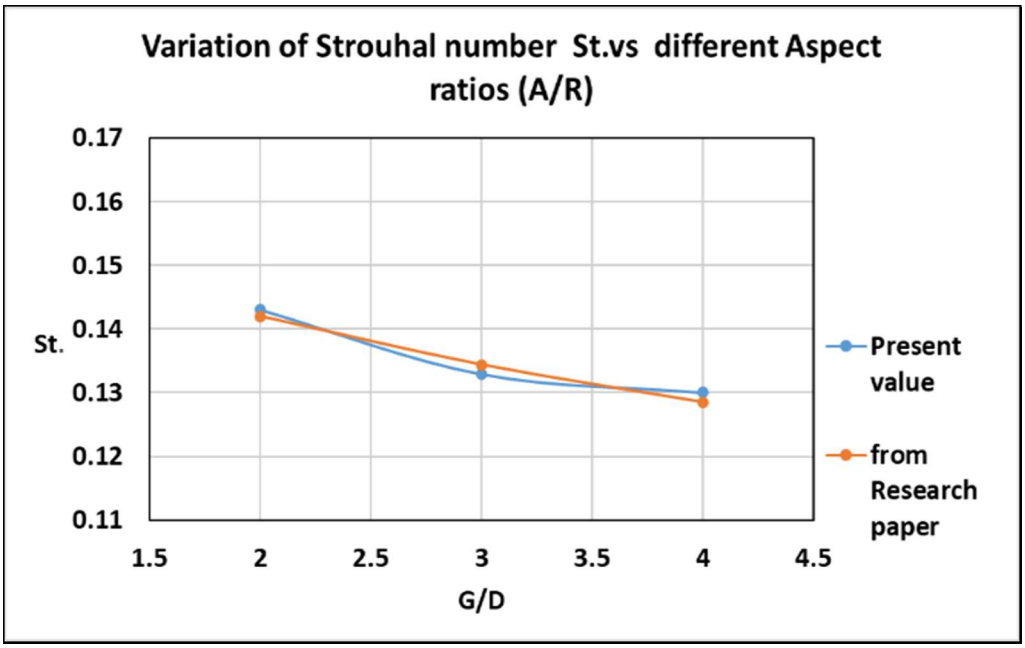


Fig. 14. Comparison of present study (blue line) and results of R. Wang et. al. for variation of Strouhal number St at different aspect ratios A/R for the uniform flow past a heated rectangular cylinder with rounded corners present between two solid wall boundaries.

A detailed comparison in the results of drag coefficient and Strouhal number at different aspect ratios has been displayed above. Above graph compares the results of R. Wang et. al. with current study based selected grid model for different aspect ratios.

3.3 Governing Equations and computational methods

For the current study, the governing equations of the incompressible fluid flow are always the continuity, Navier–Stokes and energy equation represented below.

Continuity equation,

$$\frac{\partial u}{\partial x} + \frac{\partial v}{\partial y} = 0 \qquad \text{— (1)}$$

Momentum equation,

$$\rho \left(\frac{\partial u}{\partial t} + u \frac{\partial u}{\partial x} + v \frac{\partial u}{\partial y} \right) = - \frac{\partial p}{\partial x} + \mu \left(\frac{\partial^2 u}{\partial x^2} + \frac{\partial^2 u}{\partial y^2} \right) \qquad \text{— (2)}$$

$$\rho \left(\frac{\partial v}{\partial t} + u \frac{\partial v}{\partial x} + v \frac{\partial v}{\partial y} \right) = - \frac{\partial p}{\partial y} + \mu \left(\frac{\partial^2 v}{\partial x^2} + \frac{\partial^2 v}{\partial y^2} \right) \quad \text{— (3)}$$

Energy equation,

$$\rho C_p \frac{\partial \theta}{\partial t} + \rho C_p \left(u \frac{\partial \theta}{\partial x} + v \frac{\partial \theta}{\partial y} \right) = k \left(\frac{\partial^2 \theta}{\partial x^2} + \frac{\partial^2 \theta}{\partial y^2} \right) \quad \text{— (4)}$$

where t, ρ, μ, and P represent the time, density, dynamic viscosity, and pressure of the incompressible fluid, respectively. u denotes the velocity of the fluid in the x-direction, while v represents the velocity in the y-direction.

The left-hand sides of eqns. (2) and (3) represent advection, while the first terms on the right-hand sides are the pressure gradient terms, the middle two terms on the right-hand sides of these two equations denote the shear forces resulting from fluid viscous.The solver used is a pressure based solver in ANSYSFLUENT2025R1, in which SIMPLE (Semi-implicit pressure linked equation) algorithm is used to solve the governing equations. Spatial discretization is done and second order upwind scheme is used for solving momentum and energy equation. Transient formulation is done by first order Implicit scheme.The solution is assumed to be converged when the divergence in each cell falls well below $<< 10^{-6}$.

3.4 Boundary conditions

Current study investigates a forced convection heat transfer from a rectangular cylinder located near a plane stationary wall. The study is done considering Reynolds number (Re)=100, Prandtl number (Pr) = 0.71 and the cylinder being placed at various gap ratios (G/D) ranging from 0.1 to 1 with an increment of 0.1, along with other gap ratios of (G/D) = 2,3 and 4.

At the inflow boundary a uniform flow profile is assumed. i.e., U=U_∞, V=0 and θ=0.

The top and bottom boundaries are considered to be stationary plane wall with U=0, V=0 and $\frac{\partial \theta}{\partial y}$ =0.

At the cylinder surface, non-slip conditions for the velocities and constant temperature conditions are applied on the cylinder surface. i.e.,U=0, V=0, θ =1.

Upstream length (L_{us}) = 9D

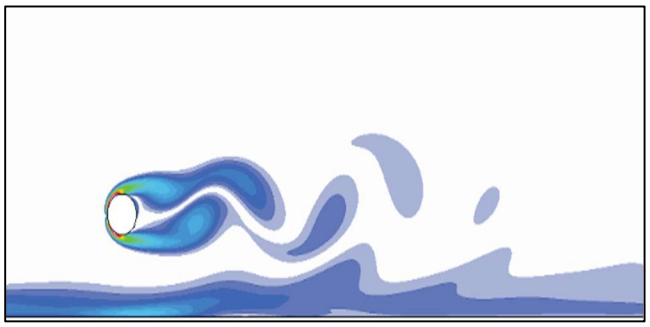
Downstream length (L_{ds}) = 19D

Chapter 4

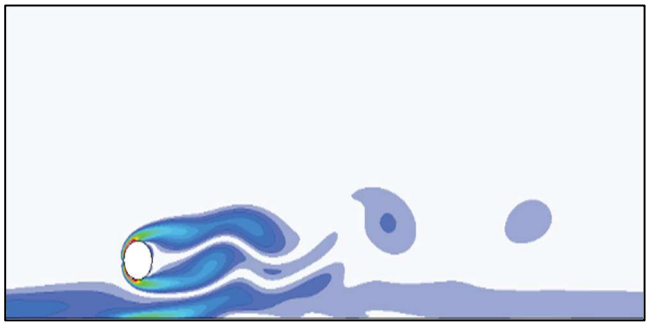
Results and Discussions

4.1 Flow characteristics

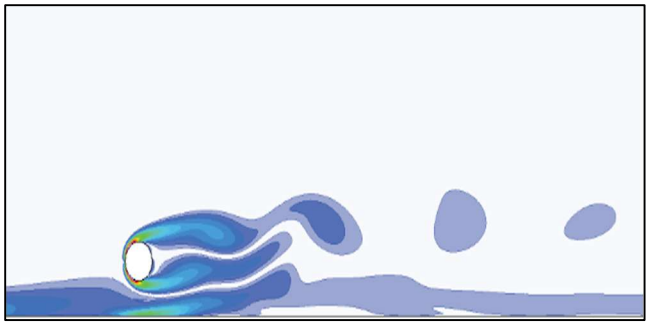
4.1.1 Time evolution of lift coefficient and drag coefficient



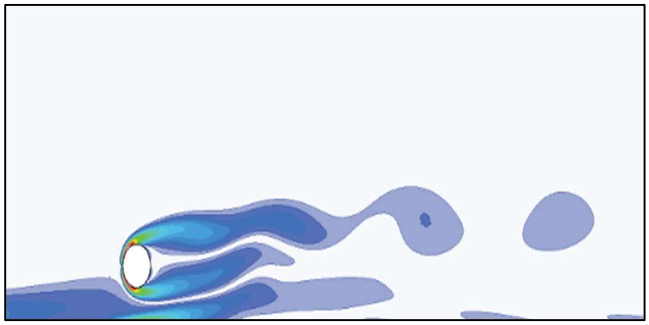
G/D = 2



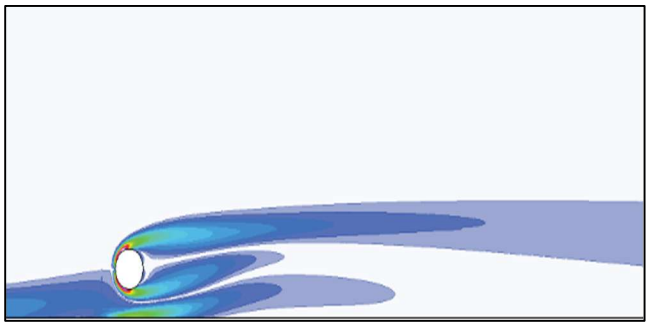
G/D = 1



G/D = 0.9

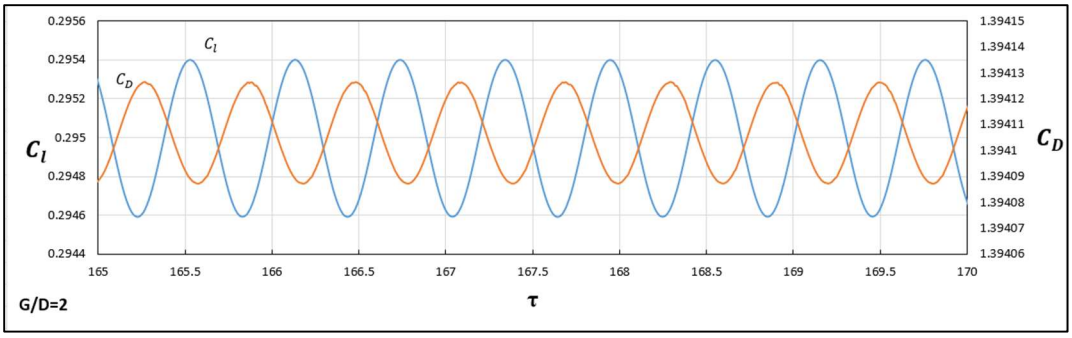


G/D = 0.8

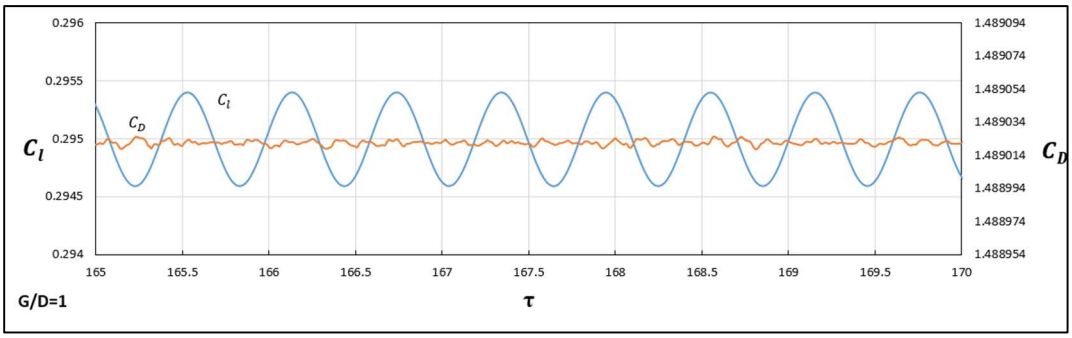


G/D = 0.7

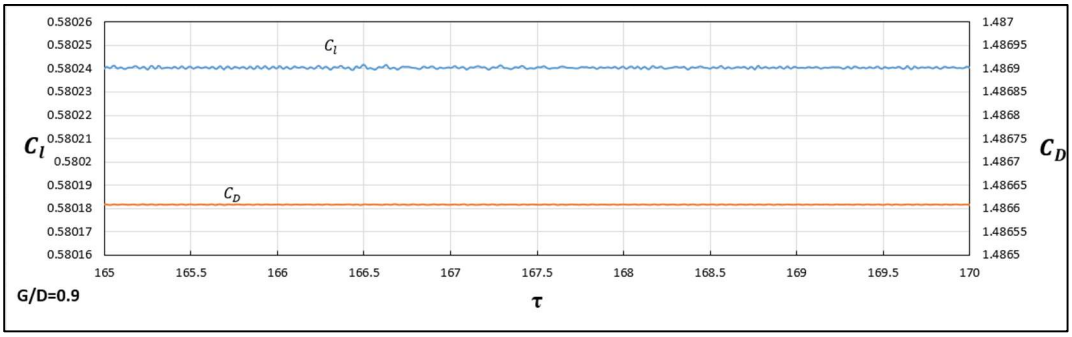
Fig.15a. Instantaneous vorticity contour for rectangular cylinder with aspect ratio A/R=1 at different gap ratios.


0.2956
0.2954
0.2952
0.295
0.2948
0.2946
0.2944
C_l
C_D
1.39415
1.39414
1.39413
1.39412
1.39411
1.3941
1.39409
1.39408
1.39407
1.39406
C_D
165
165.5
166
166.5
167
167.5
168
168.5
169
169.5
170
τ
G/D=2

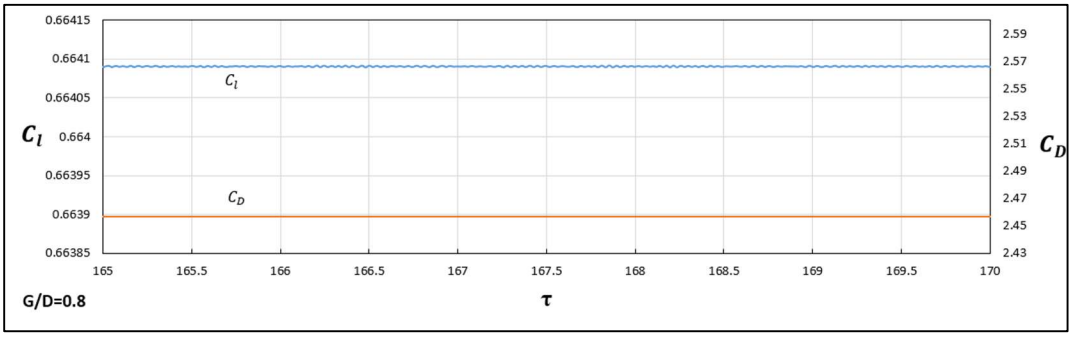
G/D = 2


0.296
0.2955
0.295
0.2945
0.294
C_l
C_D
1.489094
1.489074
1.489054
1.489034
1.489014
1.488994
1.488974
1.488954
C_D
165
165.5
166
166.5
167
167.5
168
168.5
169
169.5
170
τ
G/D=1

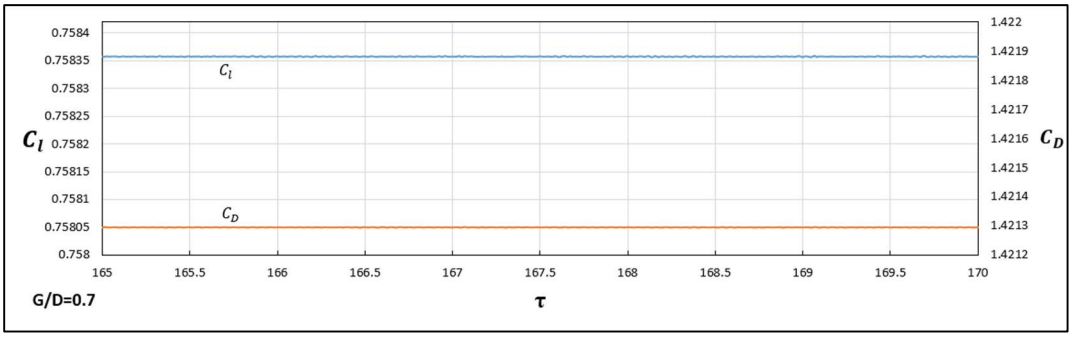
G/D = 1


0.58026
0.58025
0.58024
0.58023
0.58022
0.58021
0.5802
0.58019
0.58018
0.58017
0.58016
C_l
C_D
1.487
1.48695
1.4869
1.48685
1.4868
1.48675
1.4867
1.48665
1.4866
1.48655
1.4865
C_D
165
165.5
166
166.5
167
167.5
168
168.5
169
169.5
170
τ
G/D=0.9

G/D = 0.9


0.66415
0.6641
0.66405
0.664
0.66395
0.6639
0.66385
C_l
C_D
2.59
2.57
2.55
2.53
2.51
2.49
2.47
2.45
2.43
C_D
165
165.5
166
166.5
167
167.5
168
168.5
169
169.5
170
τ
G/D=0.8

G/D = 0.8



G/D = 0.7

Fig.15b. Time evolution of lift coefficient and drag coefficient for rectangular cylinder with aspect ratio A/R=1 at different gap ratios.

Above figure Fig 4 and Fig. 5 describes the periodic variations of the (Cd) drag coefficient (orange line) and (Cl) lift coefficient (blue line) acting on the rectangular cylinder of A/R=1 for G/D=2,1,0.9,0.8 & 0.7.

From the figure it is evident that a periodic oscillation can be observed for both the forces at higher gap ratios of G/D=2,1 compared to lower gap ratios of G/D= 0.9,0.8 & 0.7, which shows a steadier profile.

Comparing it with vorticity contour besides, it can be concluded that the nature of the wave cycle forming is a result of the alternate shedding of upper and lower vortices around the rectangular bluff body. As the body is brought closer to the stationary wall the lower vortices are seen to be suppressed and more prominent upper vortices are formed which causes a decrease in fluctuation in the nature of the wave as well as the magnitude of the forces is seen to be shifted to the upper side.

4.1.2 Instantaneous vorticity pattern

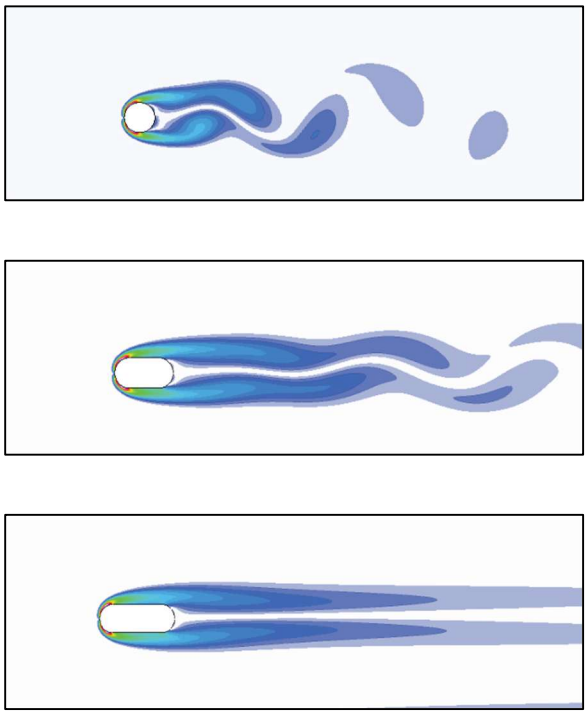
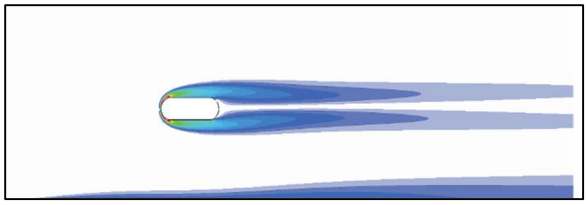


Fig. 16. Instantaneous vorticity contour for rectangular cylinder with aspect ratio A/R=1,2 & 3

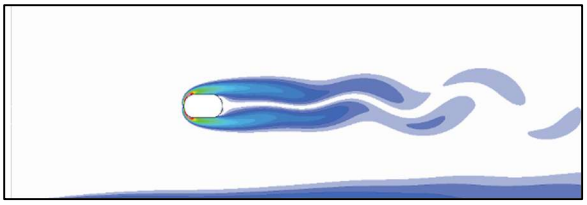
Above figure Fig. 6 shows the vorticity contours for an isolated bluff body of three different aspect ratios of A/R=1,2 & 3 in presence of flow at Re=100. It can be said that a more symmetrical wake flow pattern with greater stability can be observed for higher aspect ratio of A/R=3 to that of lower aspect ratios. For lower aspect ratios, Karman Vortex Street phenomenon can be seen prominent in the flow. As A/R increases there is an increase in the streamwise length of the cylinder which causes the stability in the corresponding flow over the body.

4.1.3 Vortex shedding during a cycle at different G/D.

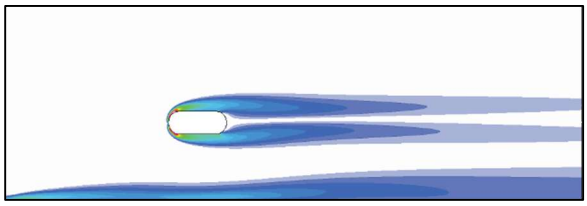
- For Aspect ratio (A/R) =3
- For Aspect ratio (A/R) =2



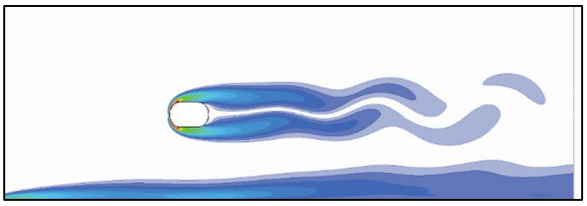
A/R 3 GD 4



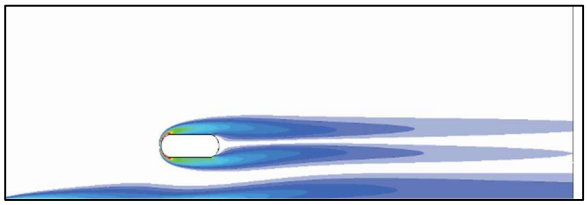
A/R 2 GD 4



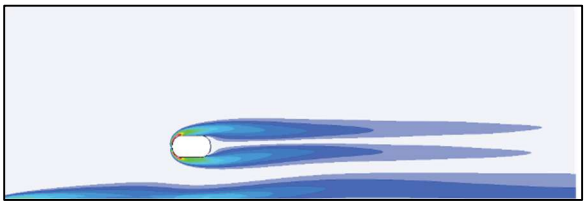
A/R 3 GD 3



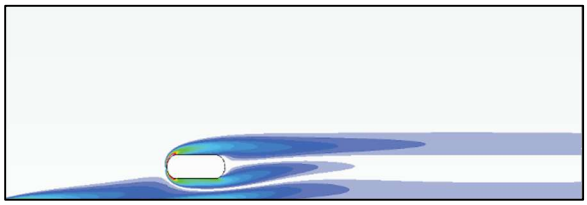
A/R 2 GD 3



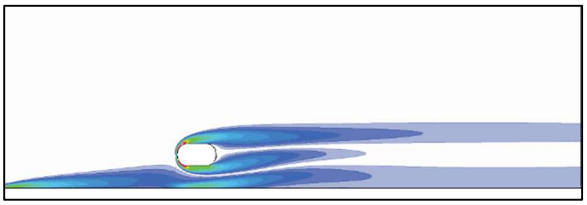
A/R 3 GD 2



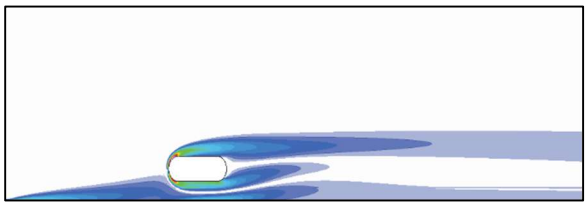
A/R 2 GD 2



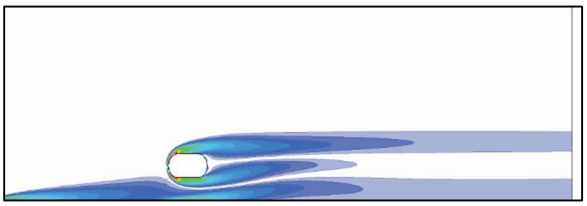
A/R 3 GD 1



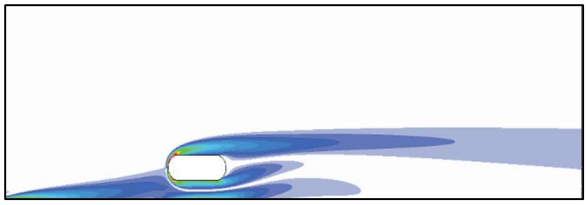
A/R 2 GD 1



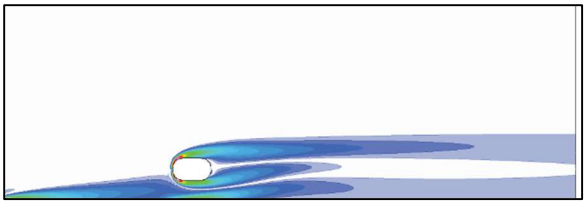
A/R 3 GD 0.9



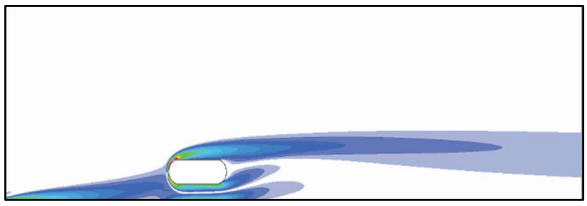
A/R 2 GD 0.9



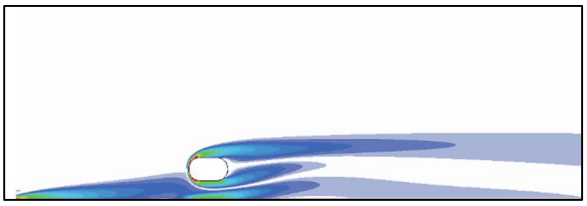
A/R 3 GD 0.8



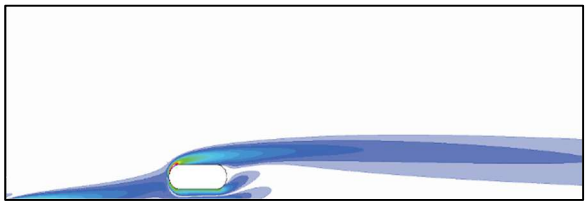
A/R 2 GD 0.8



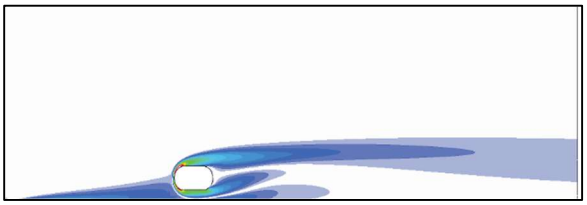
A/R 3 GD 0.7



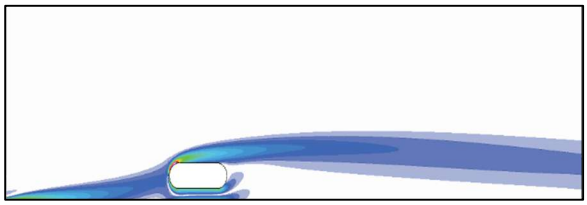
A/R 2 GD 0.7



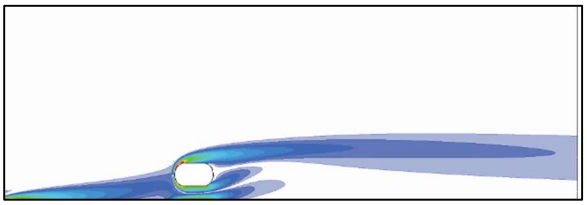
A/R 3 GD 0.6



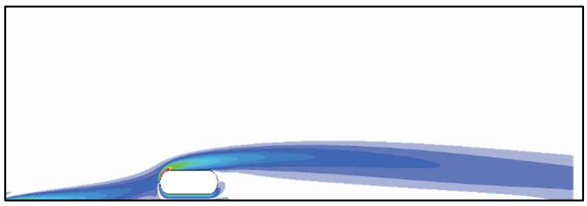
A/R 2 GD 0.6



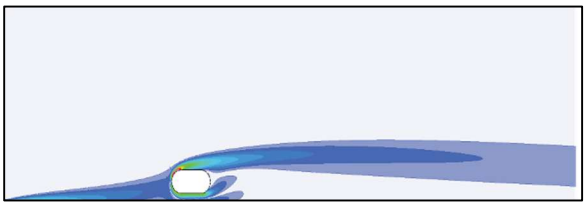
A/R 3 GD 0.5



A/R 2 GD 0.5



A/R 3 GD 0.4



A/R 2 GD 0.4

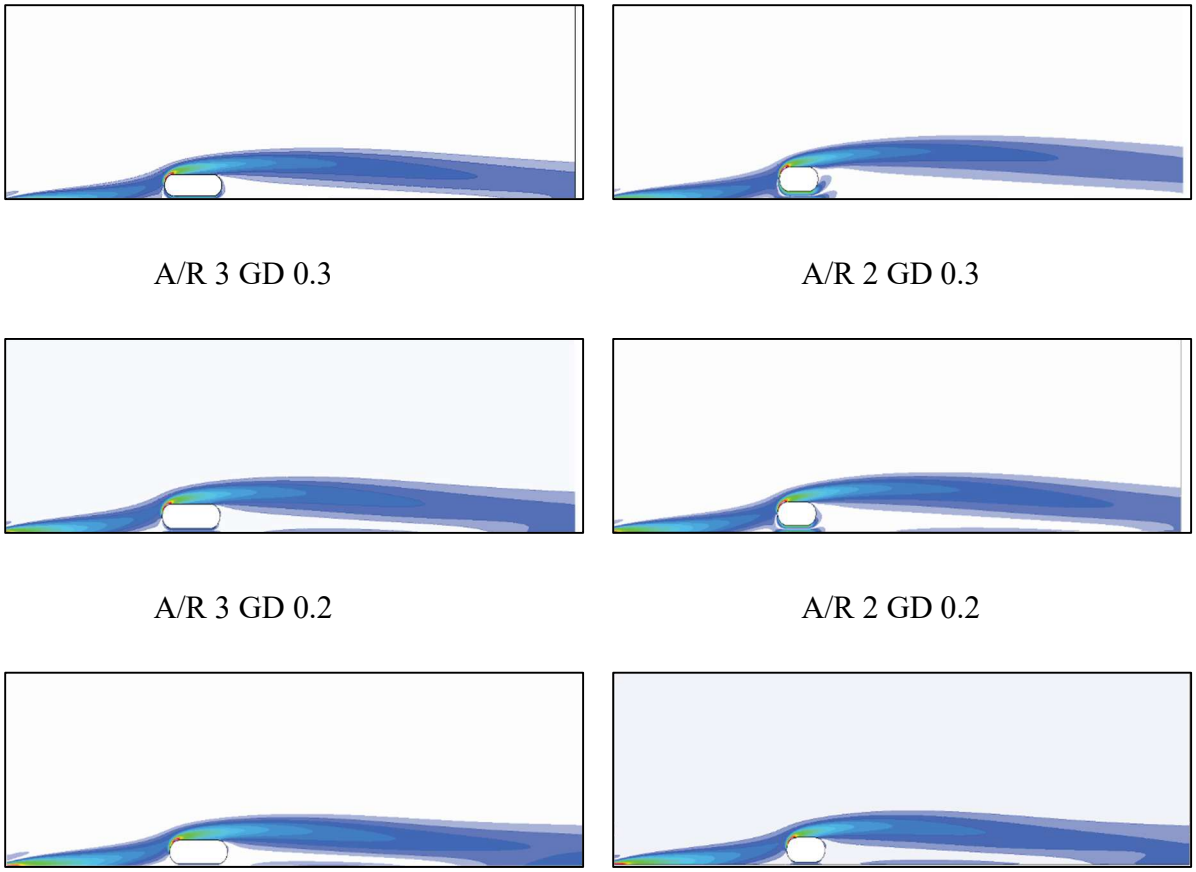


Fig. 17. Instantaneous vorticity contour for rectangular cylinder with aspect ratio A/R=2 & 3 with respect to different gap ratios.

Above figure Fig.7 depicts the variation of vorticity contours around rectangular body of Aspect ratio A/R=2 for various gap ratios G/D = 4,3,2,1,0.9,0.8,0.7,0.6,0.5,0.4,0.3,0.2 & 0.1 at Re=100. Starting from highest gap ratio of G/D=4, it can be seen that there is formation of alternate vortices shedding from the upper and lower part of the bluff body. Also some vortices can be seen to be existing along the stationary wall. For higher gap ratios like G/D = 2,3,4, there is no interaction between these vortices with the ones formed around the bluff body but as we go closer to the wall the scenario changes. Starting from G/D=1 , there can be seen an interaction between both the vortices, with decrease in length of the lower vortices of the bluff body. As we go further lower of gap ratios, the length of vortices along the wall also starts to decrease with it. With further decrease in the gap ratio of G/D=<0.6 the lower vortices of bluff body and the vortices of plane wall can be

seen to be almost equal and simultaneously the upper vortices of the bluff body starts to increase. Only upper vortices of the bluff body cease to exist for lowest gap ratios.

4.1.4 Time averaged streamlines

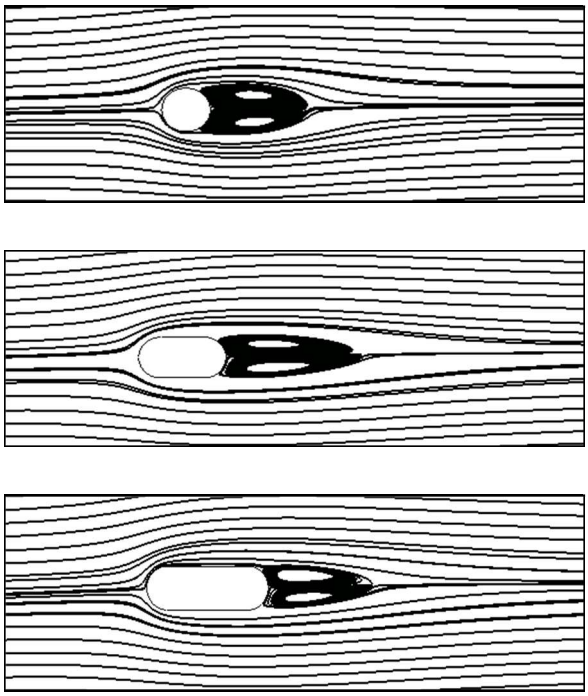
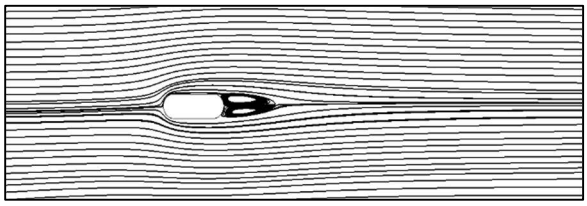


Fig. 18. Time averaged streamlines for different aspect ratios.

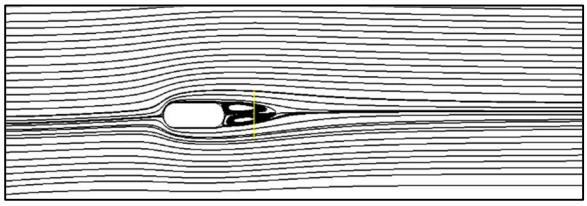
Above figure illustrates time average streamlines around the rectangular cylinder with rounded corners for different aspect ratios, considering a significant distance from the adjacent plane wall. The body with A/R=1, resembles a circular cylinder and the wake region occurring is seen to be much thicker compared to other bodies with higher aspect ratios. As aspect ratio of 2 & 3 both represent a rectangular body with rounded corners, presence of flat surface at top and bottom sides has major influence on the recirculation zones when compared with that of circular cylinder, as displayed in the figure. For starters, a much sleek wake region present within the width of the body can be observed for an aspect ratio of 2 & 3. Along with this, the wake region tends to become shorter with increasing aspect ratio, for aspect ratio of 2 & 3.

4.1.5 Time averaged velocity streamline for Aspect ratio A/R=3,2 & 1 at different G/D.

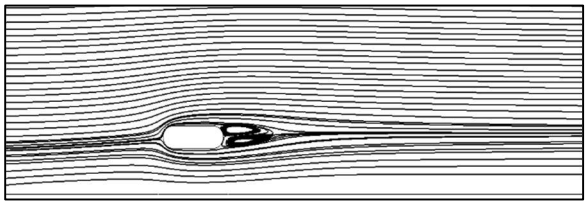
- For Aspect ratio (A/R) =3



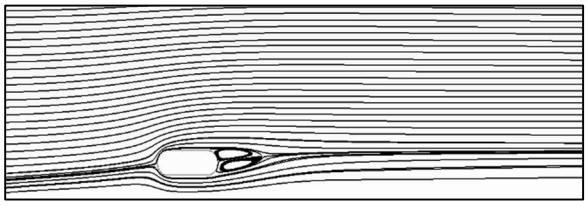
A/R 3 GD 4



A/R 3 GD 3

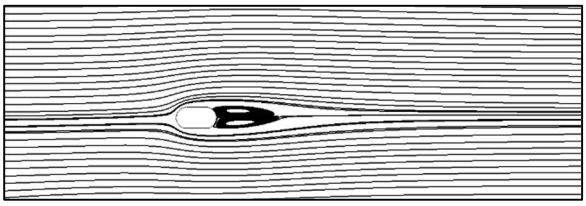


A/R 3 GD 2

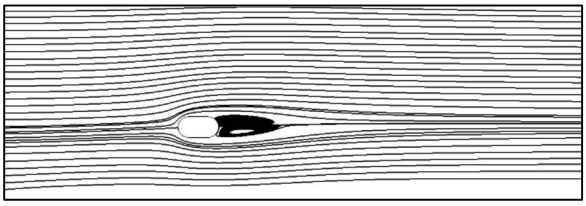


A/R 3 GD 1

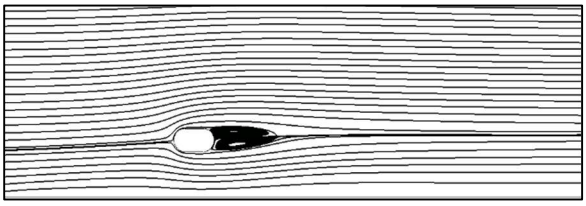
- For Aspect ratio (A/R) =2



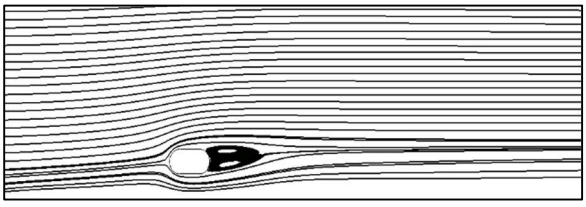
A/R 2 GD 4



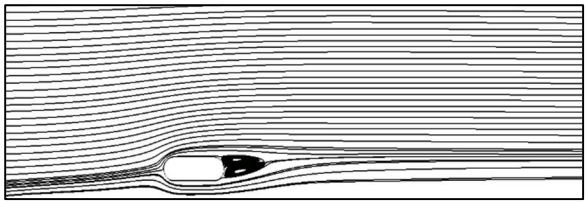
A/R 2 GD 3



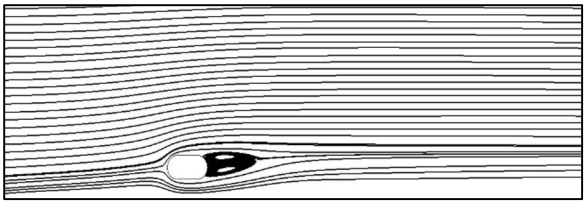
A/R 2 GD 2



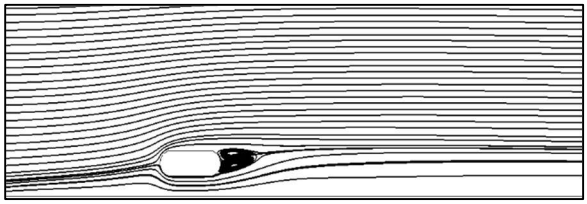
A/R 2 GD 1



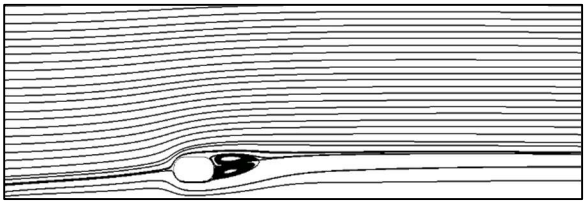
A/R 3 GD 0.9



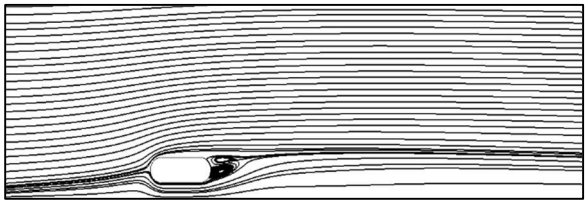
A/R 2 GD 0.9



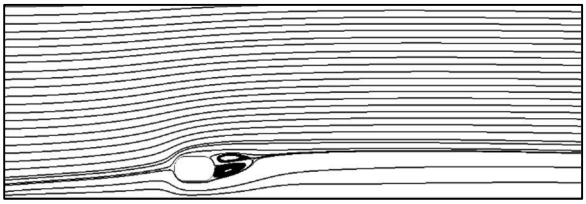
A/R 3 GD 0.8



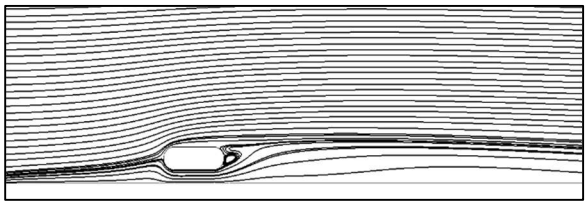
A/R 2 GD 0.8



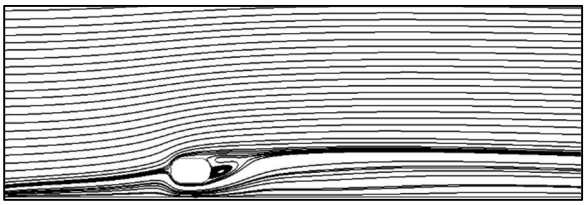
A/R 3 GD 0.7



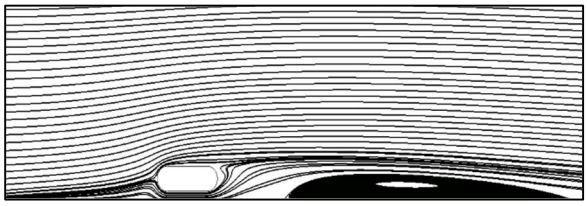
A/R 2 GD 0.7



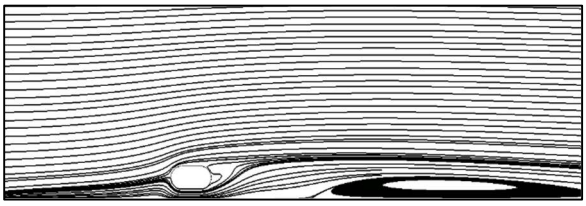
A/R 3 GD 0.6



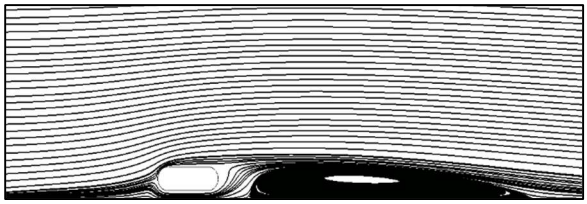
A/R 2 GD 0.6



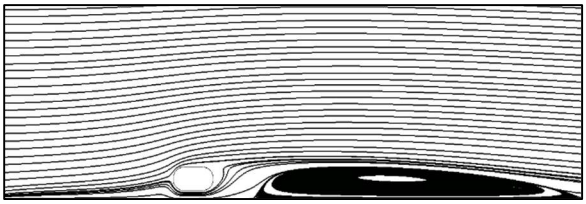
A/R 3 GD 0.5



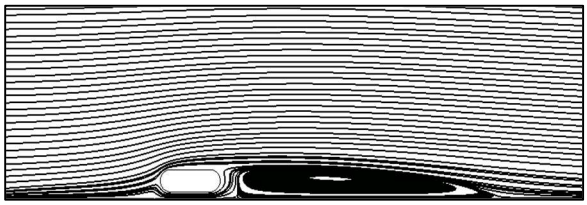
A/R 2 GD 0.5



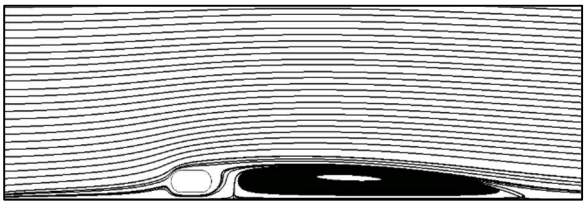
A/R 3 GD 0.4



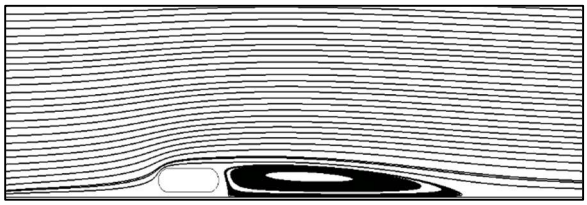
A/R 2 GD 0.4



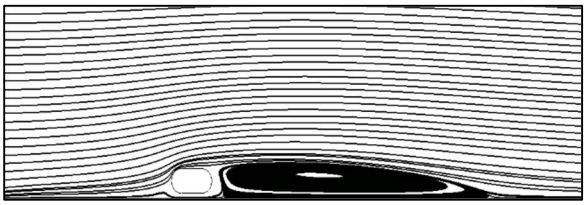
A/R 3 GD 0.3



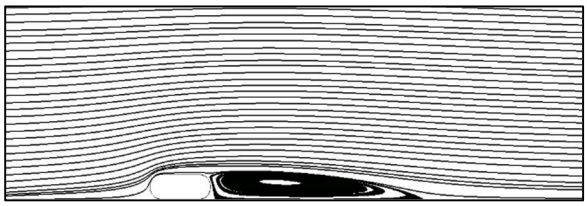
A/R 2 GD 0.3



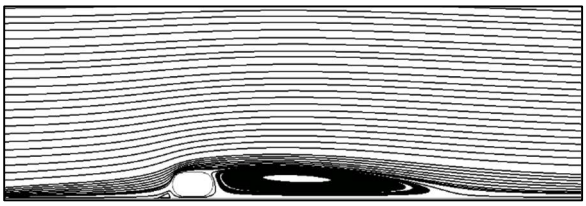
A/R 3 GD 0.2



A/R 2 GD 0.2

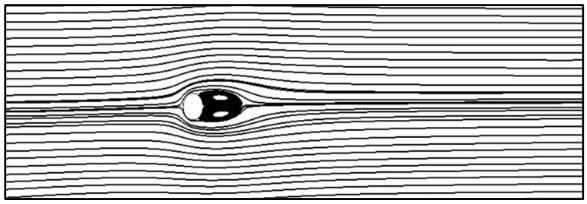


A/R 3 GD 0.1

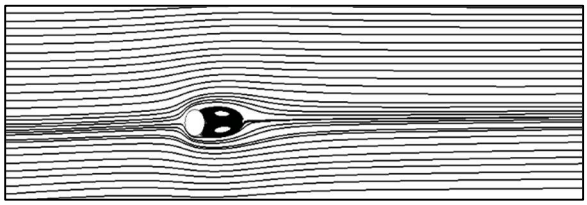


A/R 2 GD 0.1

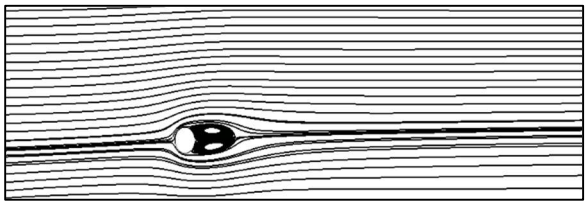
- For Aspect ratio (A/R) =1



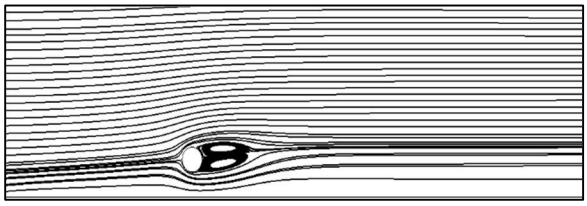
A/R 1 GD 4



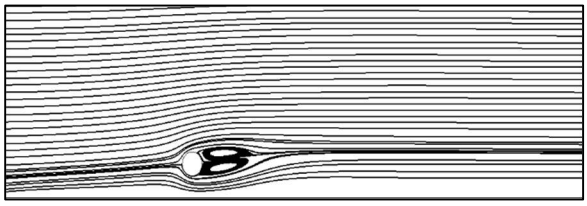
A/R 1 GD 3



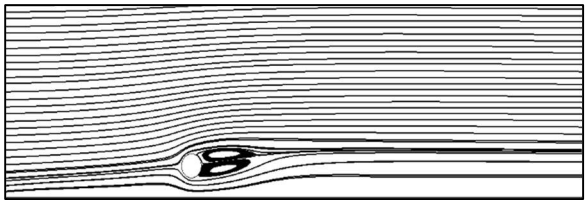
A/R 1 GD 2



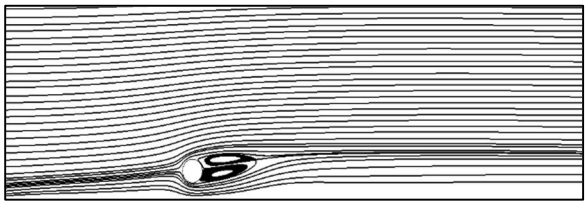
A/R 1 GD 1



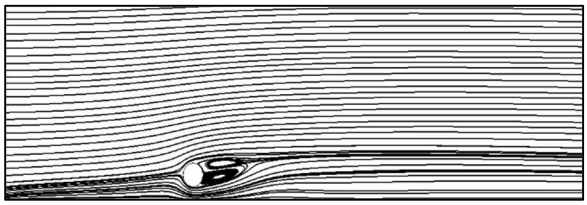
A/R 1 GD 0.9



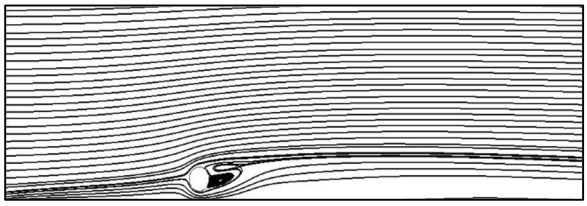
A/R 1 GD 0.8



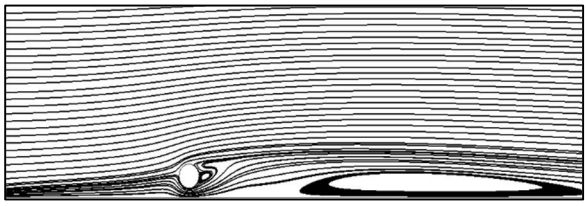
A/R 1 GD 0.7



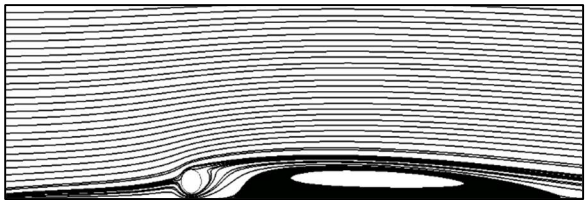
A/R 1 GD 0.6



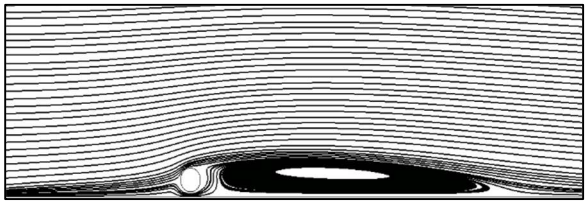
A/R 1 GD 0.5



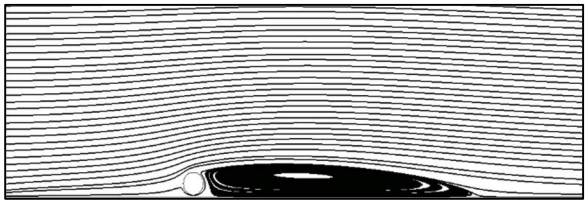
A/R 1 GD 0.4



A/R 1 GD 0.3



A/R 1 GD 0.2

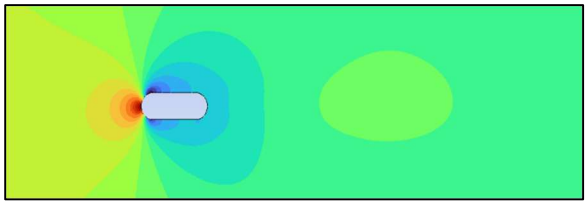


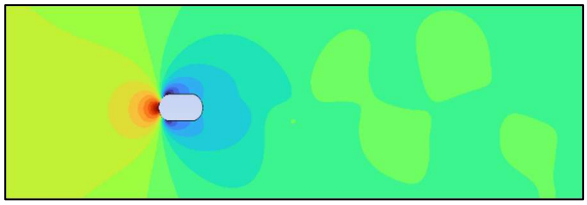
A/R 1 GD 0.1

Fig. 19. Time averaged velocity streamline for Aspect ratio A/R=3,2 & 1 at different G/D.

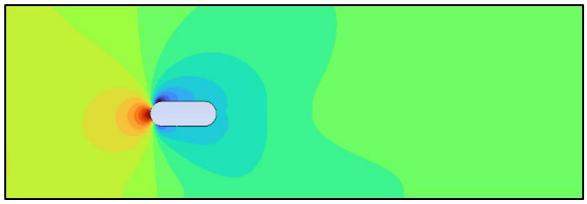
4.1.6 Pressure coefficient contour for Aspect ratio A/R=3,2 & 1 at different G/D.

- For Aspect ratio (A/R) =3
- For Aspect ratio (A/R) =2

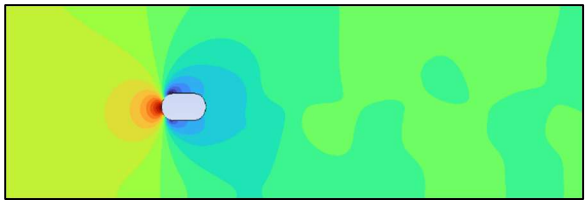




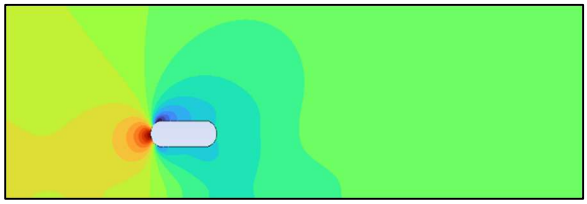
A/R 3 GD 4



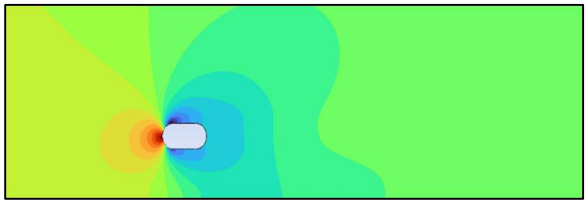
A/R 2 GD 4



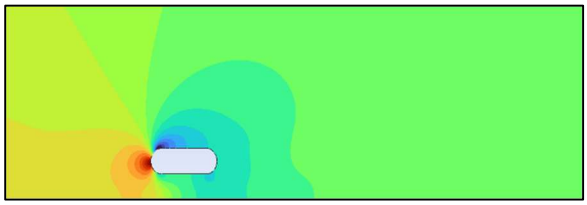
A/R 3 GD 3



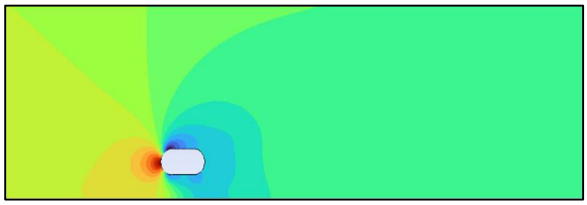
A/R 2 GD 3



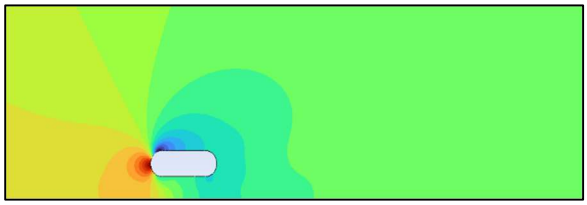
A/R 3 GD 2



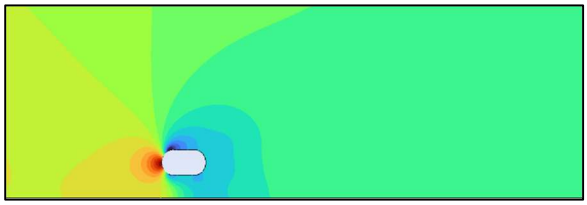
A/R 2 GD 2



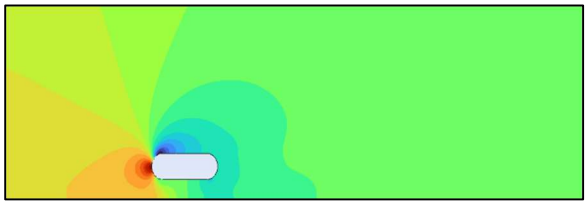
A/R 3 GD 1



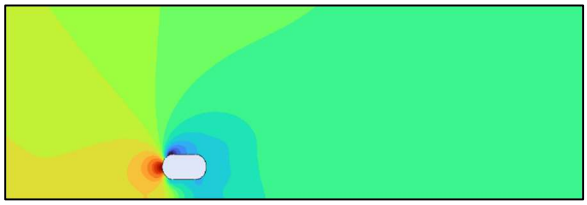
A/R 2 GD 1



A/R 3 GD 0.9

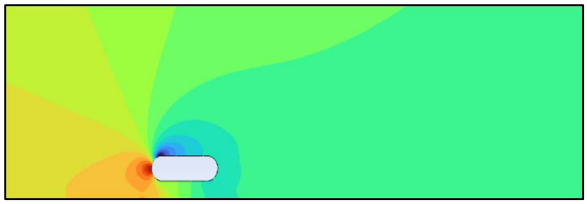


A/R 2 GD 0.9

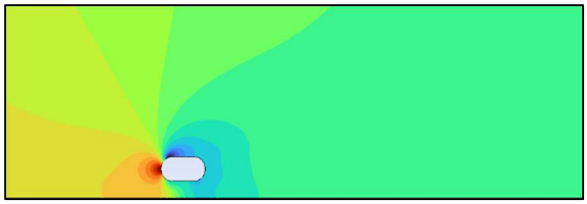


A/R 3 GD 0.8

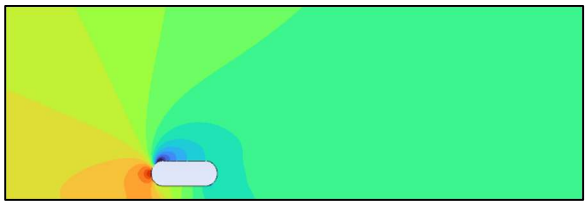
A/R 2 GD 0.8



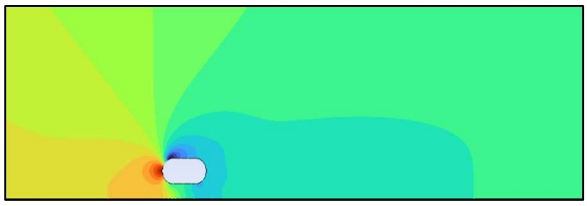
A/R 3 GD 0.7



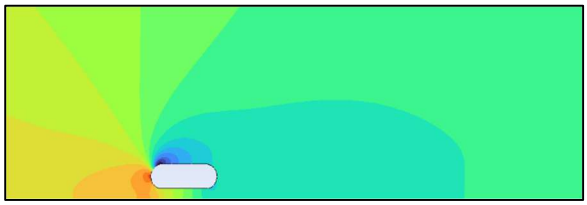
A/R 2 GD 0.7



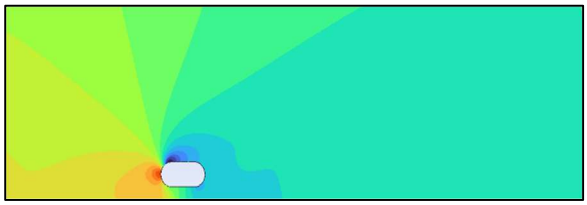
A/R 3 GD 0.6



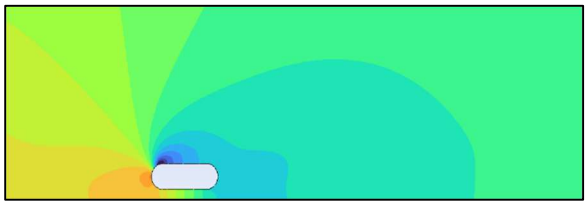
A/R 2 GD 0.6



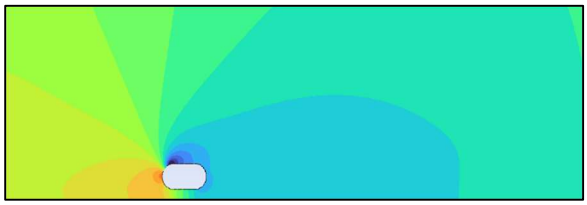
A/R 3 GD 0.5



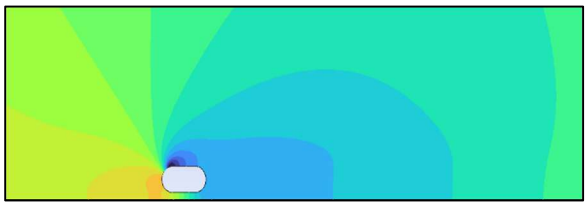
A/R 2 GD 0.5



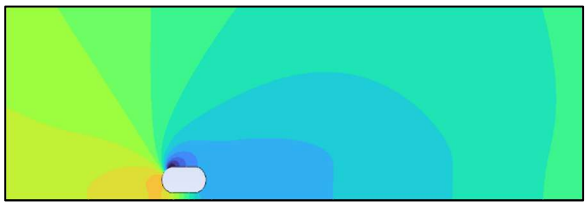
A/R 3 GD 0.4



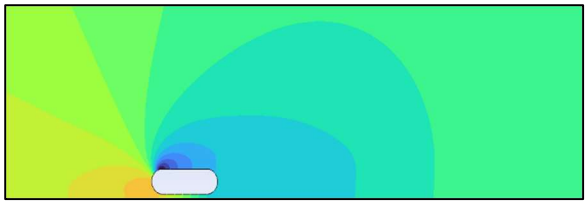
A/R 2 GD 0.4



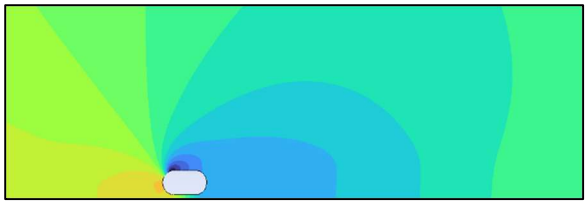
A/R 3 GD 0.3



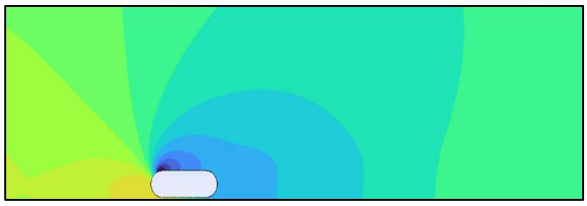
A/R 2 GD 0.3



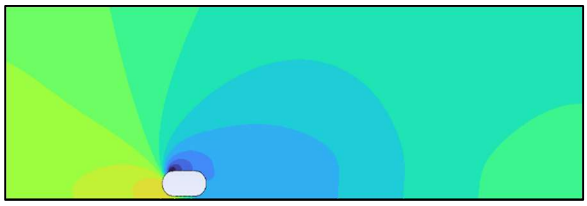
A/R 3 GD 0.2



A/R 2 GD 0.2

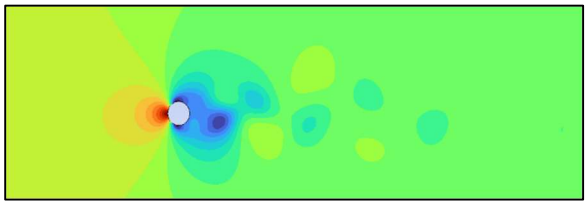


A/R 3 GD 0.1

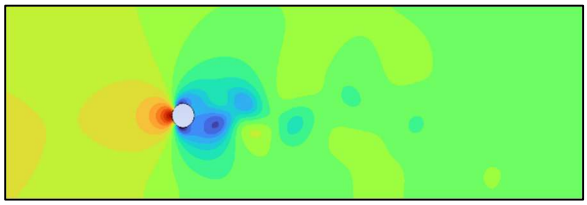


A/R 2 GD 0.1

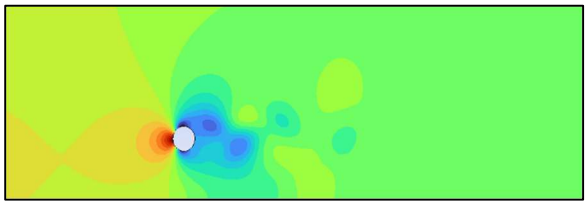
- For Aspect ratio (A/R) =1



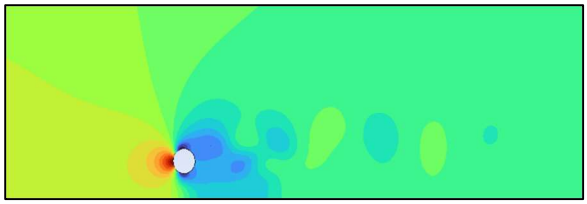
A/R 1 GD 4



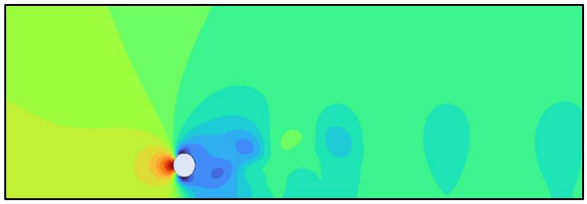
A/R 1 GD 3



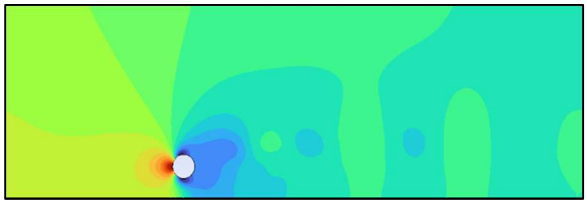
A/R 1 GD 2



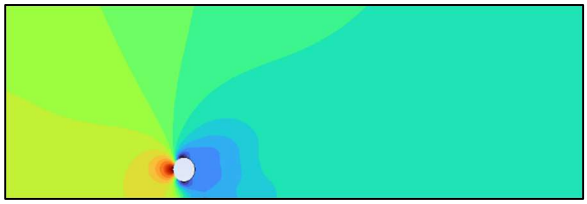
A/R 1 GD 1



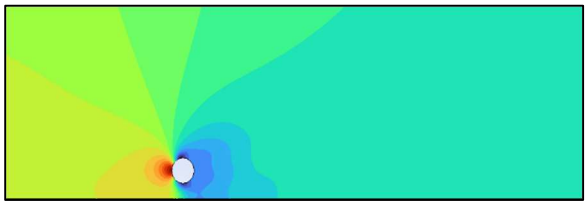
A/R 1 GD 0.9



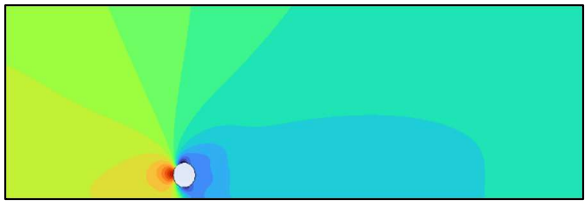
A/R 1 GD 0.8



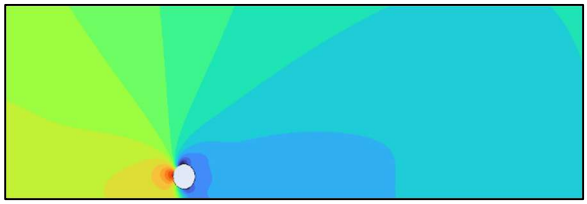
A/R 1 GD 0.7



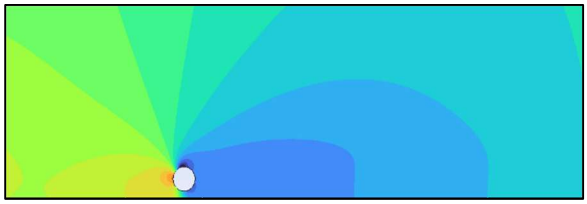
A/R 1 GD 0.6



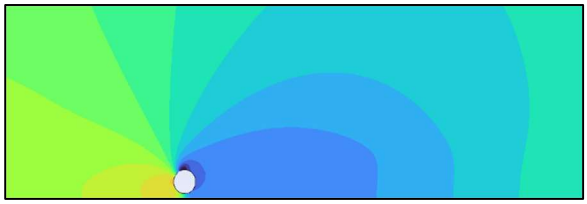
A/R 1 GD 0.5



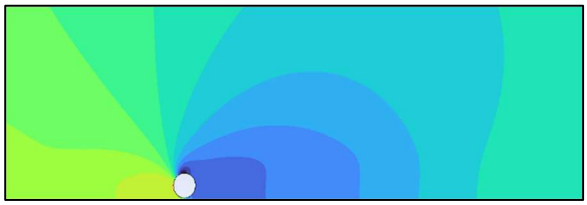
A/R 1 GD 0.4



A/R 1 GD 0.3



A/R 1 GD 0.2

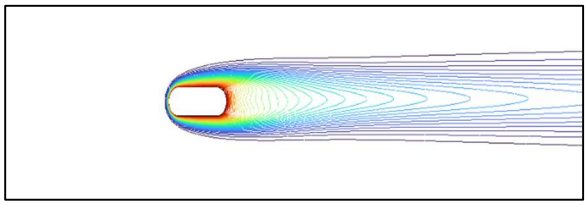


A/R 1 GD 0.1

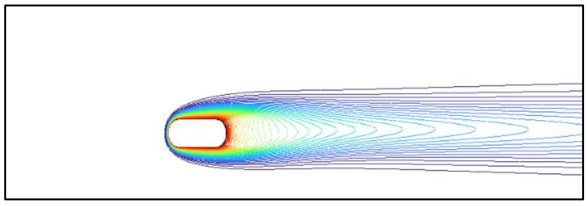
Fig. 20. Pressure coefficient contour for Aspect ratio A/R=3,2 & 1 at different G/D.

4.1.7 Isotherms for Aspect ratio A/R=3,2 & 1 during a cycle at different G/D.

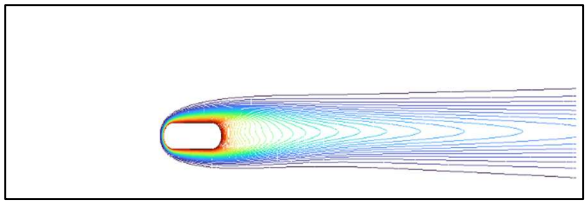
- For Aspect ratio (A/R) =3



A/R 3 GD 4

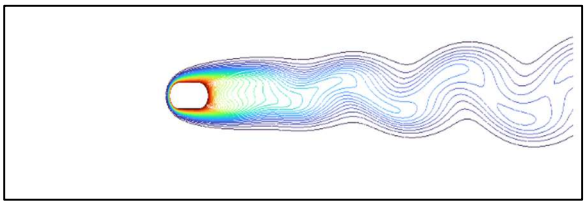


A/R 3 GD 3

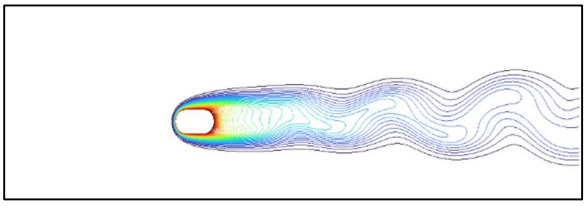


A/R 3 GD 2

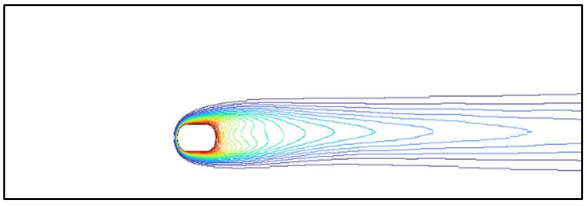
- For Aspect ratio (A/R) =2



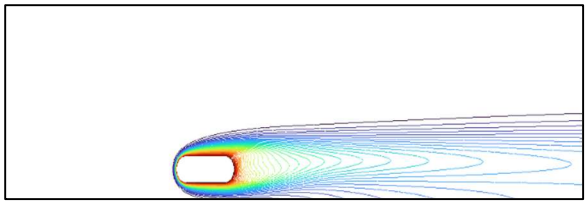
A/R 2 GD 4



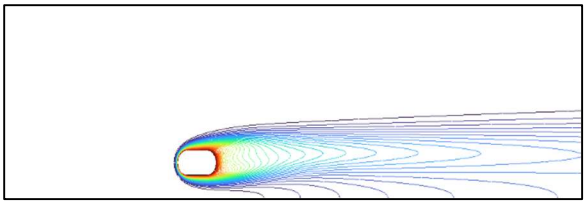
A/R 2 GD 3



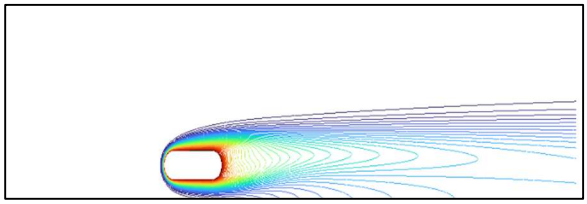
A/R 2 GD 2



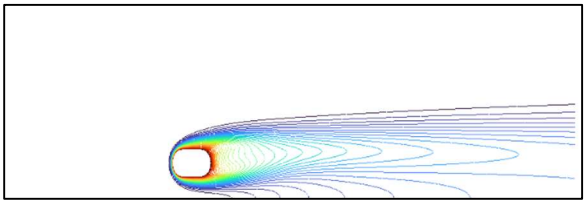
A/R 3 GD 1



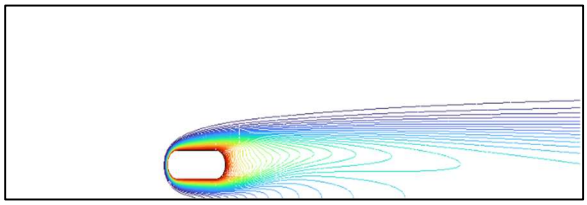
A/R 2 GD 1



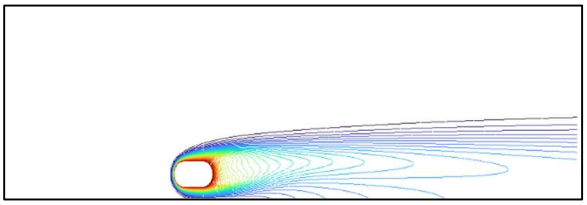
A/R 3 GD 0.9



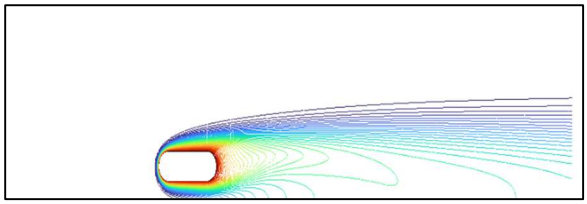
A/R 2 GD 0.9



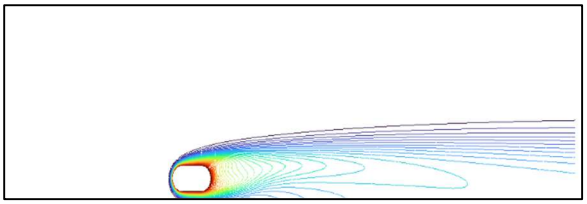
A/R 3 GD 0.8



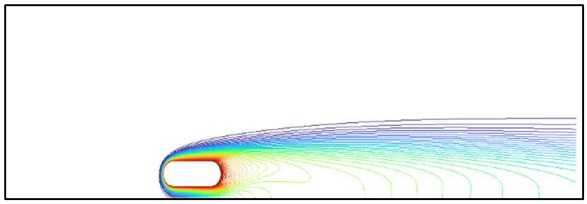
A/R 2 GD 0.8



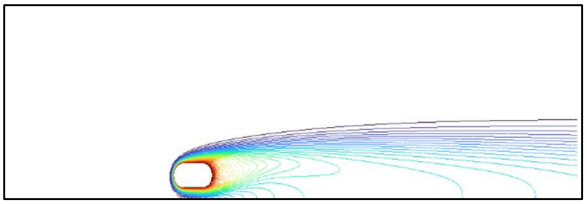
A/R 3 GD 0.7



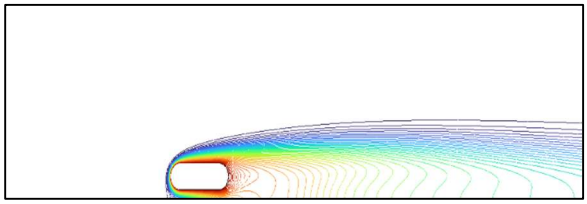
A/R 2 GD 0.7



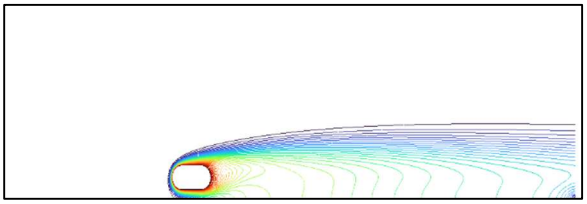
A/R 3 GD 0.6



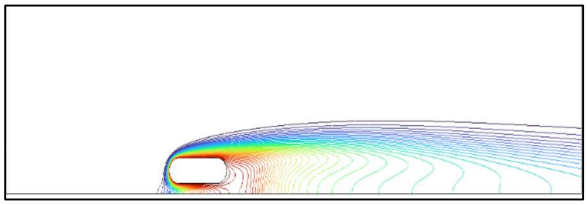
A/R 2 GD 0.6



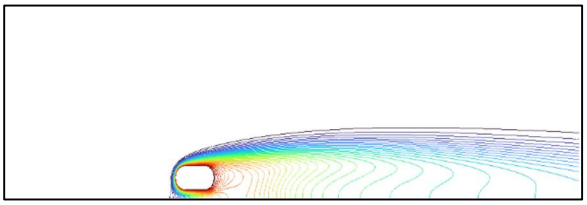
A/R 3 GD 0.5



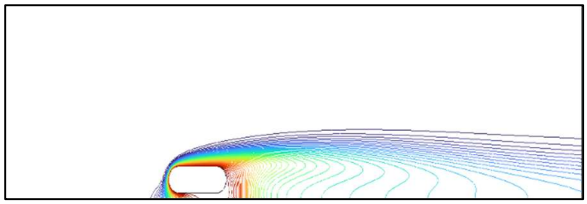
A/R 2 GD 0.5



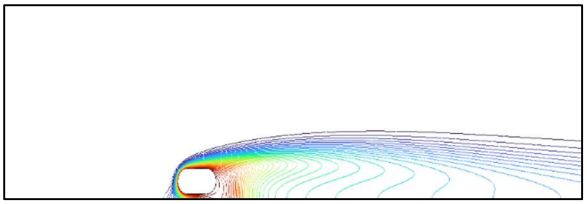
A/R 3 GD 0.4



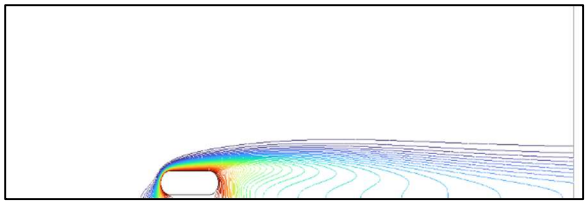
A/R 2 GD 0.4



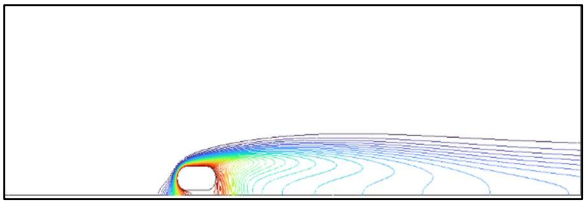
A/R 3 GD 0.3



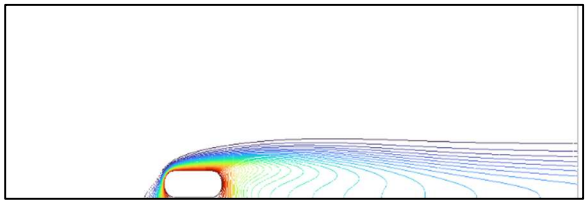
A/R 2 GD 0.3



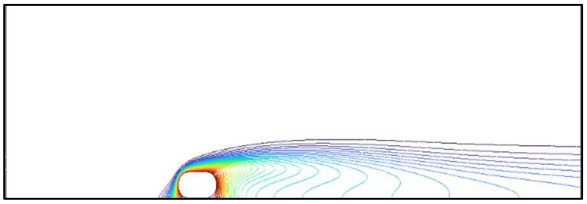
A/R 3 GD 0.2



A/R 2 GD 0.2

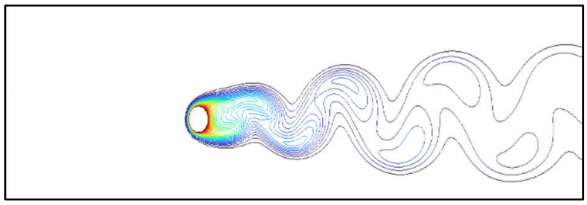


A/R 3 GD 0.1

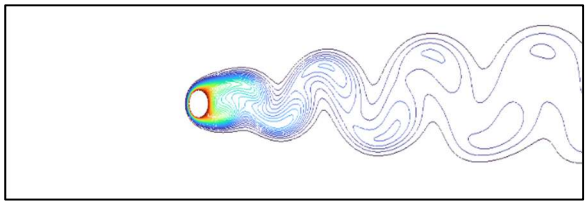


A/R 2 GD 0.1

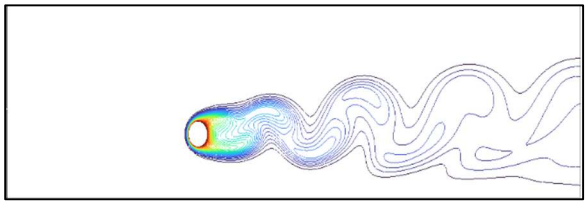
- For Aspect ratio (A/R) =1



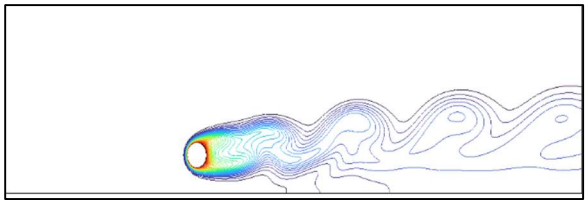
A/R 1 GD 4



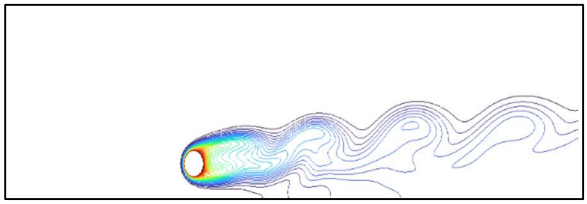
A/R 1 GD 3



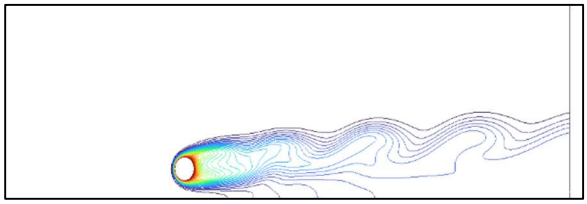
A/R 1 GD 2



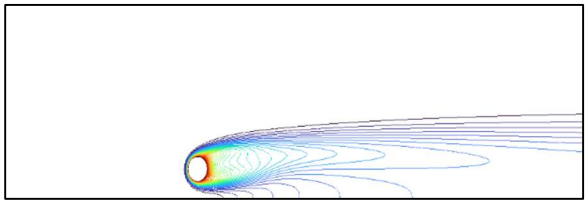
A/R 1 GD 1



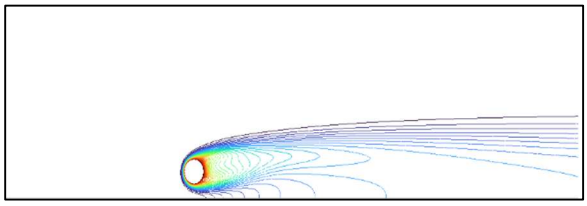
A/R 1 GD 0.9



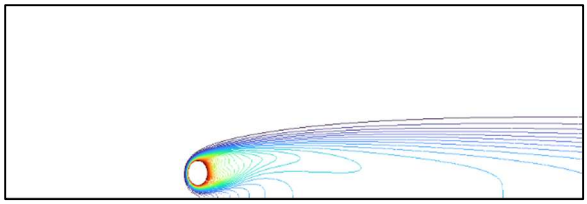
A/R 1 GD 0.8



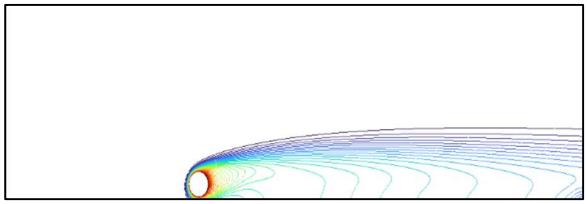
A/R 1 GD 0.7



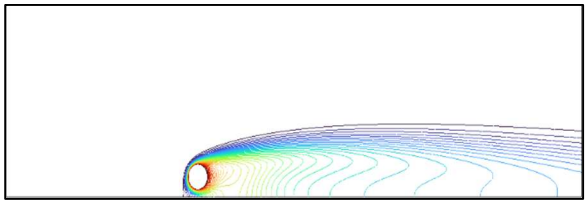
A/R 1 GD 0.6



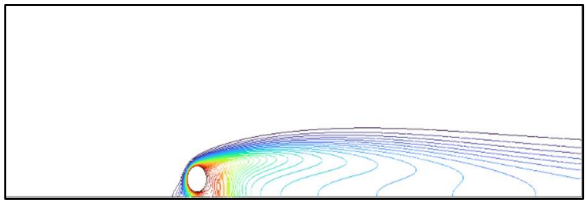
A/R 1 GD 0.5



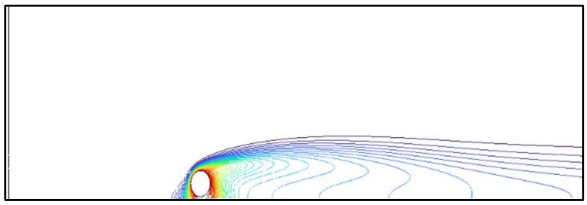
A/R 1 GD 0.4



A/R 1 GD 0.3



A/R 1 GD 0.2



A/R 1 GD 0.1

Fig. 21. Isotherms for Aspect ratio A/R=3,2 & 1 during a cycle at different G/D.

4.2 Drag Coefficients

In fluid dynamics, drag is described as the resistance exerted by a fluid against any object moving relative to it. Drag is the result of interaction between the fluid and the object's surface. It should be noted that unlike other types of resistances, drag forces are dependent on the speed of the object's movement through the medium. In laminar flow, the drag force depends linearly on the speed, but in case of turbulent flow, the drag force depends on the square of the speed.

Drag coefficient (Cd) is a dimensionless value describing drag forces acting on an object immersed into the fluid. It is defined as the drag force divided by the product of the dynamic pressure of the fluid multiplied by reference area. Drag coefficient (Cd) is normally evaluated experimentally. It depends on the form of an object and the nature of flow past the body. For example, for a smooth streamlined body, drag coefficient (Cd) will be lower than for an irregularly shaped body. The drag coefficient (Cd) formula is given by

$$C_D = \frac{F_D}{\frac{1}{2}\rho_\infty A V_\infty^2}$$

where F_D is the drag force, ρ_∞ is the fluid density, $V_\infty$is the fluid velocity, and A is the reference area.

4.2.1 Time averaged Drag coefficient (Cd)

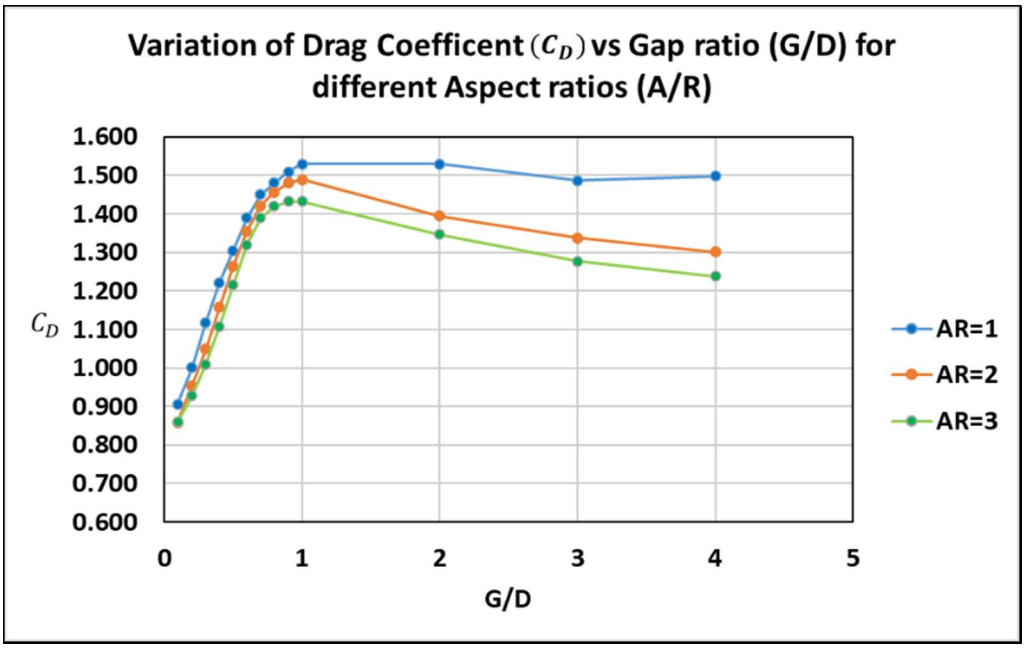


Fig. 22. Variation of mean Drag coefficient CD vs gap ratio for different aspect ratio of A/R = 1,2 & 3.

Above figure Fig. 8 illustrates how the drag coefficient (Cd) varies with the gap ratios for different aspect ratios of bluff bodies, with the Reynolds number (Re) set at 100. For the rectangular bluff body, the drag coefficient (Cd) remains relatively for gap ratios greater than 1 than for less than 1. At a gap ratio of 1, the drag coefficient (Cd) is seen to be maximum for the respective aspect ratios i.e. about 1.53,1.489 and 1.432 for the aspect ratios of 1,2 and 3 respectively . As we further decrease the gap ratio, a steep decrease in drag coefficient (Cd) can be observed going as low as 0.85 for aspect ratios of 2 & 3.Although not much of a difference in drag coefficient (Cd) can be seen in between different gap ratios for lower gap ratios. This pattern indicates that the rectangular bluff body is more sensitive to changes in the gap ratio when it is below 1 with very less influence of aspect ratio for the same range, but for higher gap ratios an observable difference can be identified with respect to aspect ratios.

4.3 Lift Coefficients

The lift coefficient (Cl) is yet another dimensionless parameter that can be used to quantify the effect of lift force on an object in a fluid medium. The lift coefficient (Cl) is the ratio of lift force to dynamic pressure multiplied by reference area. The lift coefficient (Cl) is important in

aerodynamics and fluid dynamics as it helps quantify the lift on bodies like wings and airfoils.The lift coefficient (Cl) formula is given by:

$$C_l = \frac{F_l}{\frac{1}{2}\rho_\infty A V_\infty^2}$$

Where F_l is the lift force, ρ_∞ is the fluid density, V_∞ is the fluid velocity, and A is the reference area. In conclusion, the drag coefficient (Cd) and lift coefficient (Cl) are key components in the field of fluid mechanics when analyzing and predicting the performance of objects in a fluid flow situation. With these coefficients, it is possible to design efficient structures.

4.3.1 Time averaged Lift coefficient (Cl)

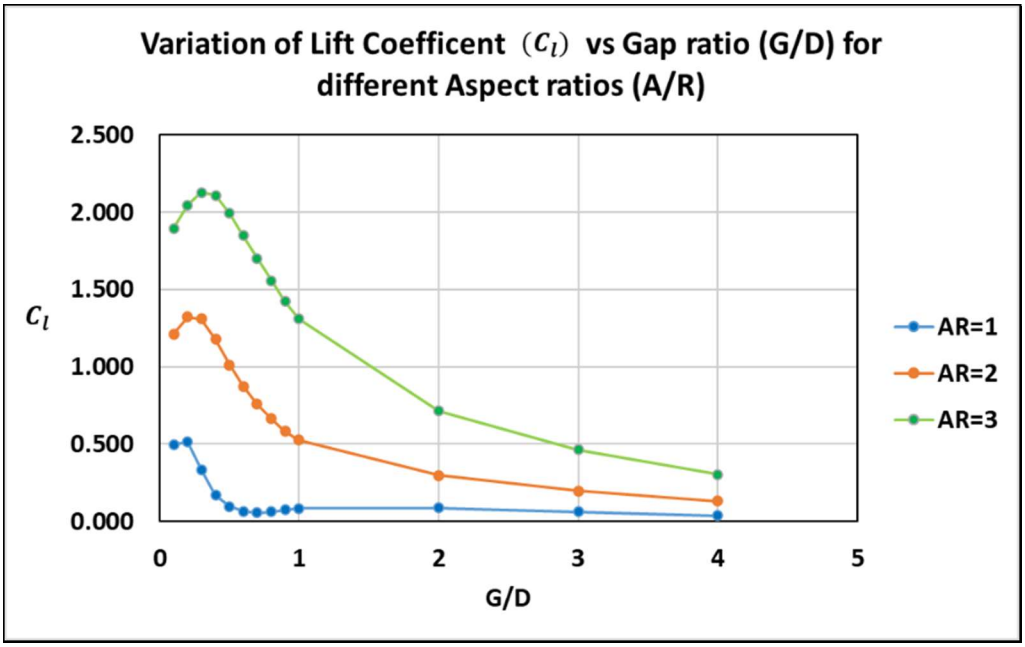


Fig. 23. Variation of mean Lift coefficient Cl vs gap ratio for different aspect ratio of A/R = 1,2 & 3.

Above figure Fig. 9 depicts the variation of the time averaged lift coefficient (Cl) at different gap ratios for rectangular bluff bodies of three different aspect ratios, with the Reynolds number (Re) consistently set at 100. This setup allows for a direct comparison of how each body of different aspect ratio responds to changes in the gap ratio under the same flow conditions. For the rectangular bluff body, there is a slow increase in the lift coefficient (Cl) as the gap ratio decreases.

At a gap ratio of 0.2 for aspect ratio 1 & 2 and a gap ratio of 0.3 for aspect ratio of 3, the lift coefficient (Cl) is seen to be maximum. As the gap ratio further decreases the lift coefficient (Cl) is further seen to decrease. Unlike drag coefficient (Cd), for all three aspect ratios high variation in lift coefficient (Cl) can be seen for lower gap ratios than at higher gap ratio and the difference between the values are seen to be decreasing as the gap ratios increase.

4.4 Pressure coefficient (Cp)

Pressure coefficient (Cp) being a dimensionless number gives the relative pressure at a point in fluid flow compared to the free stream pressure with respect to the dynamic pressure of the flow. It is a dimensionless quantity used in fluid mechanics to show how the pressure at a point compares with the free-stream pressure. It can be defined as: -

$$C_p = \frac{p - p_\infty}{\frac{1}{2}\rho_\infty V_\infty^2}$$

where p is the local static pressure, p_∞ is the free-stream pressure, ρ_∞ is the free-stream density, and V_∞ is the free-stream velocity. In simple terms, C_p tells whether the pressure at a point is higher or lower than the surrounding flow pressure. A positive value means the local pressure is higher than free stream, while a negative value means the pressure is lower. In CFD and aerodynamic studies, pressure coefficient is very important for analysing pressure distribution around bluff bodies, aerofoils, and other surfaces. The main reason being the gap between the body and the plane wall. Further understanding of the variation can be studied with the help of the given figure below Fig. 10, Fig. 11 and Fig. 12, which shows the variation of pressure coefficient (Cp) along the surface of the cylinder.

4.4.1 Distribution of time averaged pressure coefficient (Cp) on the surface of the square cylinder for A/R=1,2,& 3 .

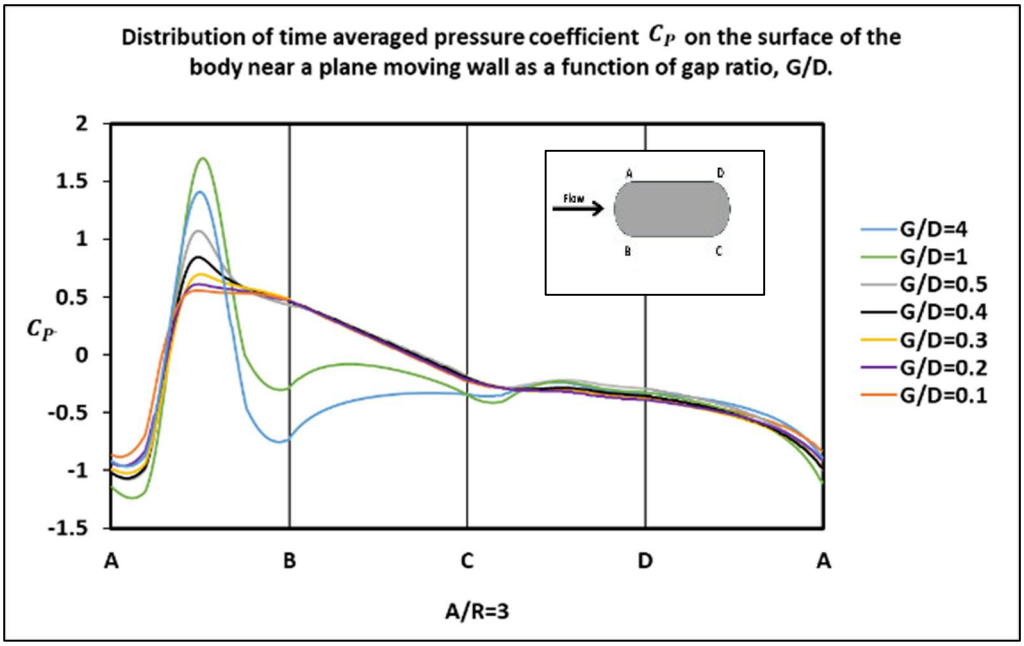


Fig. 24. Distribution of time averaged pressure coefficient Cp on the surface of the body of aspect ratio A/R=3 near a stationary wall as a function of gap ratio, G/D.

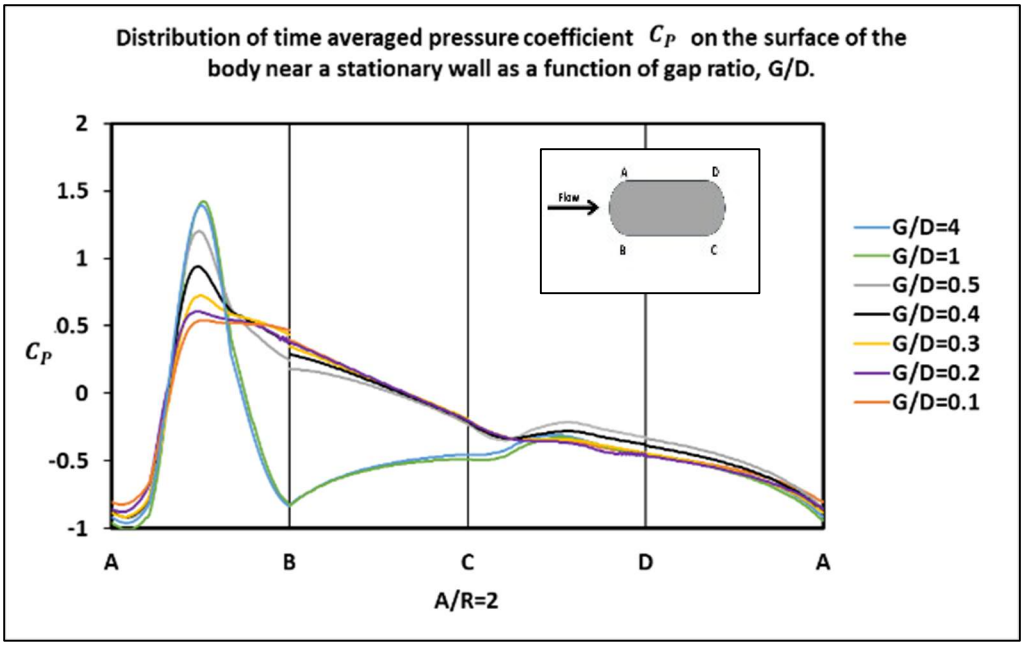


Fig. 25. Distribution of time averaged pressure coefficient Cp on the surface of the body of aspect ratio A/R=2 near a stationary wall as a function of gap ratio, G/D.

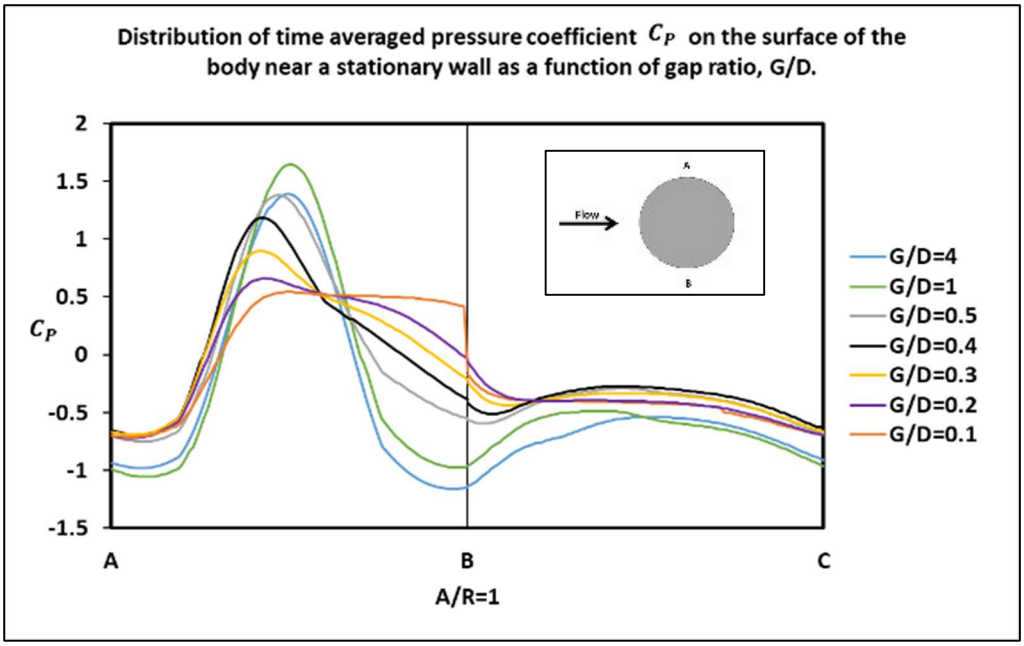


Fig. 26. Distribution of time averaged pressure coefficient Cp on the surface of the body of aspect ratio A/R=1 near a stationary wall as a function of gap ratio, G/D.

Compared to front and bottom surfaces, the top rear surface shows a stable and less variation in pressure coefficient (Cp) magnitude for different gap ratios. A clear distinction between the values at different gap ratios can be seen for front and bottom surfaces. The highest peak in the magnitude of pressure coefficient (Cp) lies in the front region and this peak decreases in magnitude with decreasing gap ratio i.e as the body comes closer to the plane wall. Averaging the magnitude for individual surface we get the following figure shown below Fig. 13, Fig. 14 and Fig. 15

4.4.2 Average Pressure coefficient (Cp) along the faces of rectangular cylinders for A/R=1,2 & 3.

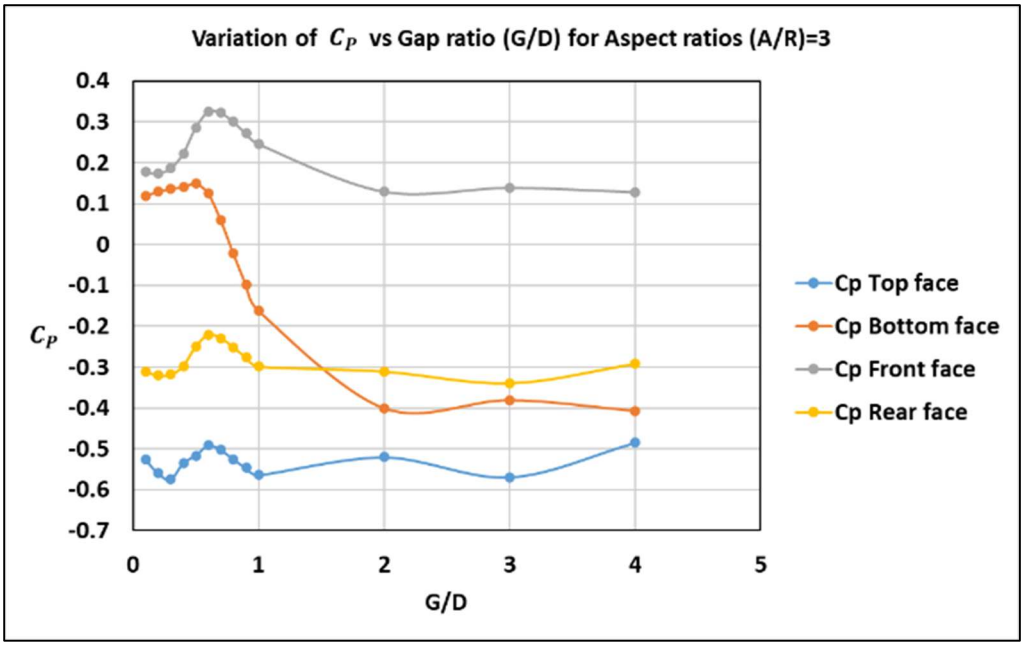


Fig. 27. Average Pressure coefficient (Cp) along the faces of rectangular cylinders for A/R=3 at different gap ratios G/D.

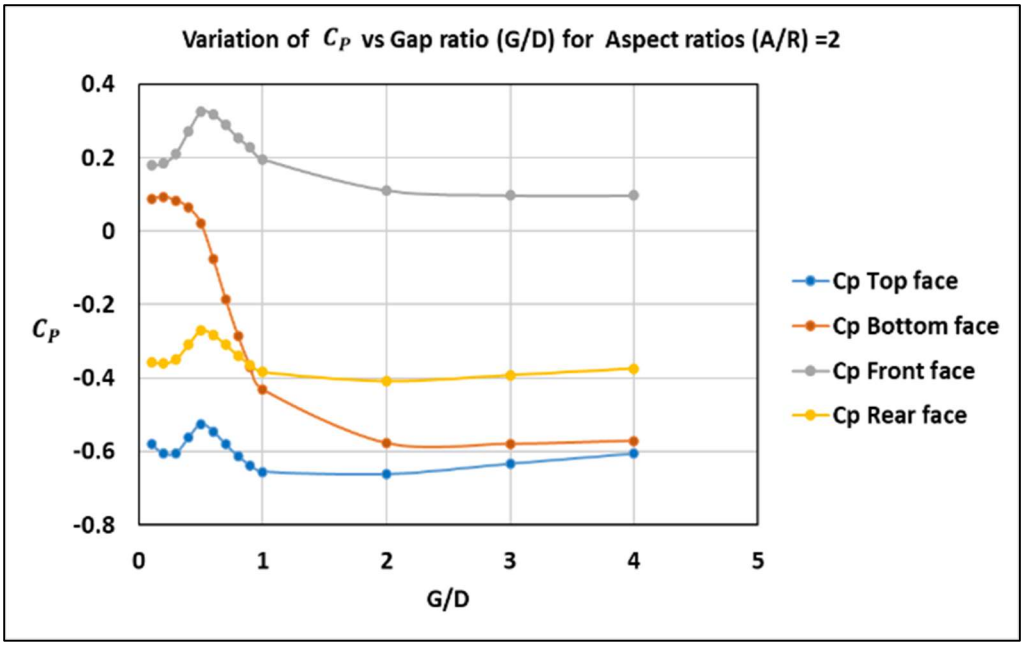


Fig. 28. Average Pressure coefficient (Cp) along the faces of rectangular cylinders for A/R=2 at different gap ratios G/D.

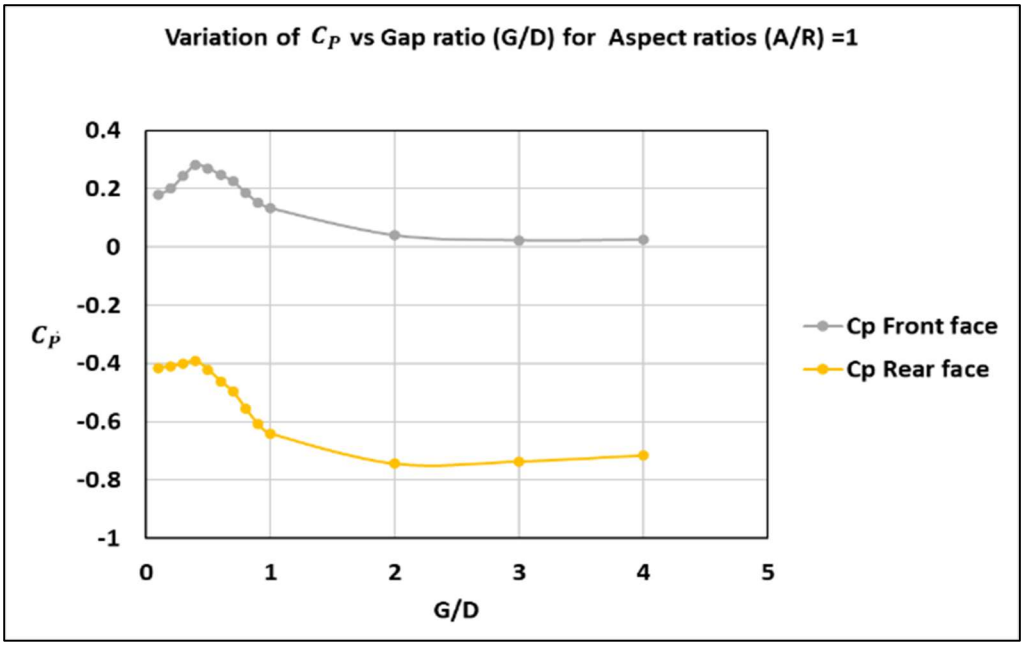


Fig. 29. Average Pressure coefficient (Cp) along the faces of rectangular cylinders for A/R=1 at different gap ratios G/D.

Similar to the case of average Nusselt number (Nu), highest range of average pressure coefficient (Cp) can be seen for front surface region with top surface being on the lower side for A/R of 2 & 3. Other than the bottom surface, all other surfaces show a stable graph with a slight change on the lower gap ratios. Whereas a huge rise in the magnitude can be seen for bottom surface as it approaches the gap ratios lower to 1.

4.4.3 Mean Pressure coefficient

Below figure Fig. 16 shows the relation between average pressure coefficient (Cp) of the rectangular of different aspect ratio with its gap ratios with respect to the plane wall.

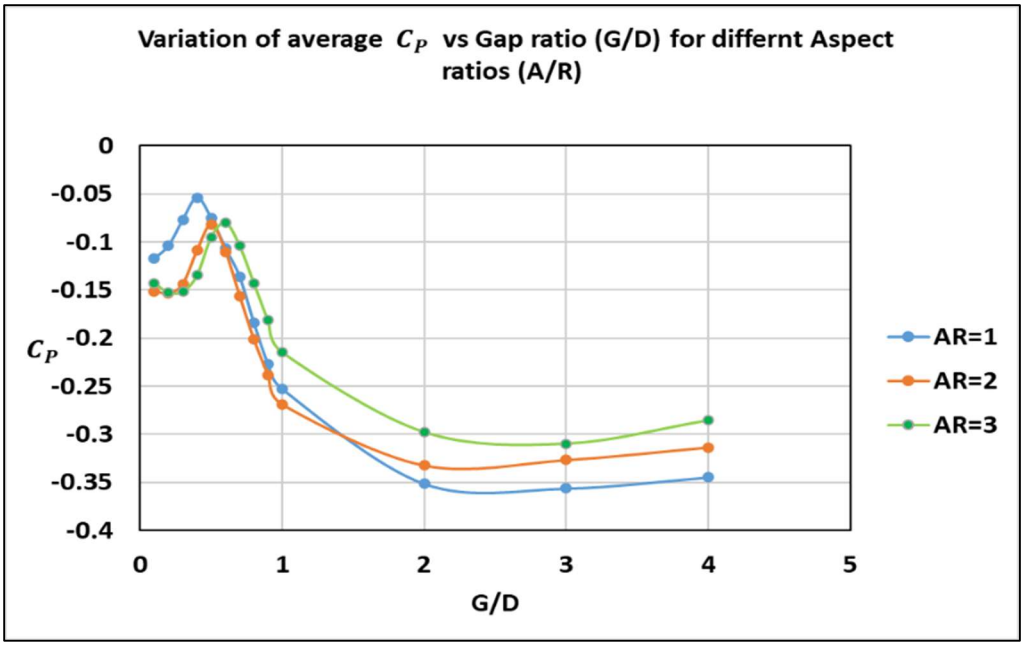


Fig. 30. Variation of mean Pressure coefficient Cp vs gap ratio for different aspect ratio of A/R = 1,2 & 3.

It is very clear that there is a rise in magnitude of the average pressure coefficient (Cp) as the gap ratio decreases irrespective of the aspect ratio, peaking at gap ratio close to 0.4 and again starting to decrease with lower gap ratios. For g/d =>2, a clear distinction in pressure coefficient (Cp) between different aspect ratios can be seen with lower A/R being on the lower side and vice versa. As G/D decreases from 2, A/R=1 tends to rise at a higher rate compared toA/R=2 and crosses it at G/D=1.5 with A/R=3 still being on the top of both of them.

4.5 Strouhal number

The Strouhal number (St) is a dimensionless parameter used in fluid dynamics to describe the unsteady behaviour of fluid flow around an object. It is used in fluid mechanics to describe oscillating flow, especially vortex shedding behind bluff bodies. It quantifies the relationship between the frequency of vortex shedding or oscillations in the flow and the flow velocity, along with a characteristic length scale of the object.

the Strouhal number (St) is expressed as:

$$St = \frac{fL}{U},$$

Where f represents the frequency of vortex shedding or flow oscillations, L is a characteristic length scale of the object (such as its diameter or width), and U is the flow velocity.

In simple terms, the Strouhal number tells how often vortices are shed relative to the flow speed and body size. It is very important in bluff body flows because it helps predict unsteady behaviour and flow-induced vibrations. For a cylinder and similar bluff bodies, the Strouhal number is often used to analyse wake dynamics and vortex shedding patterns. In CFD and experimental studies, it is a key parameter for comparing flow behaviour across different geometries and flow conditions.

In the figure given below Fig. 17, the graph depicts the variation of the Strouhal number (St) with the different gap ratios for aspect ratio of 1 rectangular bluff bodies, maintaining a constant Reynolds number (Re) of 100.

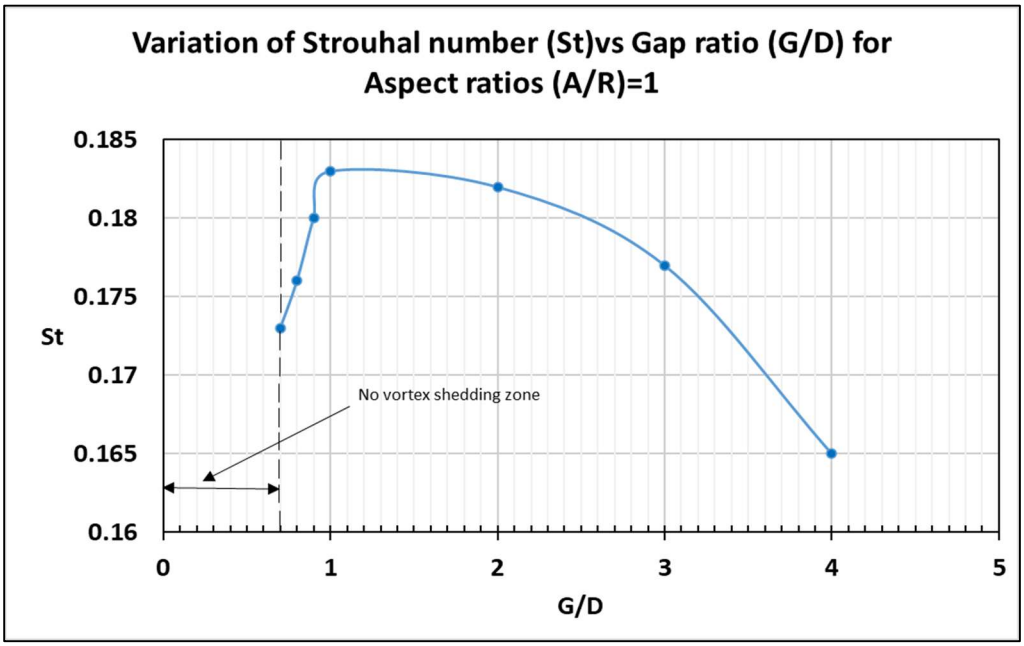


Fig. 31. Variation of Strouhal number St vs gap ratio for aspect ratio of A/R = 1.

For 4<=G/D=<1, as the gap ratio decreases to 1, the Strouhal number (St) is seen to increase reaching a maximum point at a gap ratio of 1. At a gap ratio of 1, the Strouhal number (St) is about 0.183 for rectangular bluff bodies. This value steadily drops to around 0.173 as the gap ratios reaches to 0.7. The data reveals that despite the decreasing gap ratios after 0.7, the Strouhal

numbers (St) for rectangular bluff bodies cease to exist as there is suppression of vortex shedding due to adjacent plane wall.

4.6 Recirculation length

The recirculation length is the distance from the rear of a bluff body to the point where the flow reattaches or the streamwise velocity becomes positive again. This region, often called a recirculation zone which is characterized by reversed flow and vortex formation and it plays a critical role in momentum, heat, and mass transfer in fluid systems, as well as in flame stabilization in combustion applications.

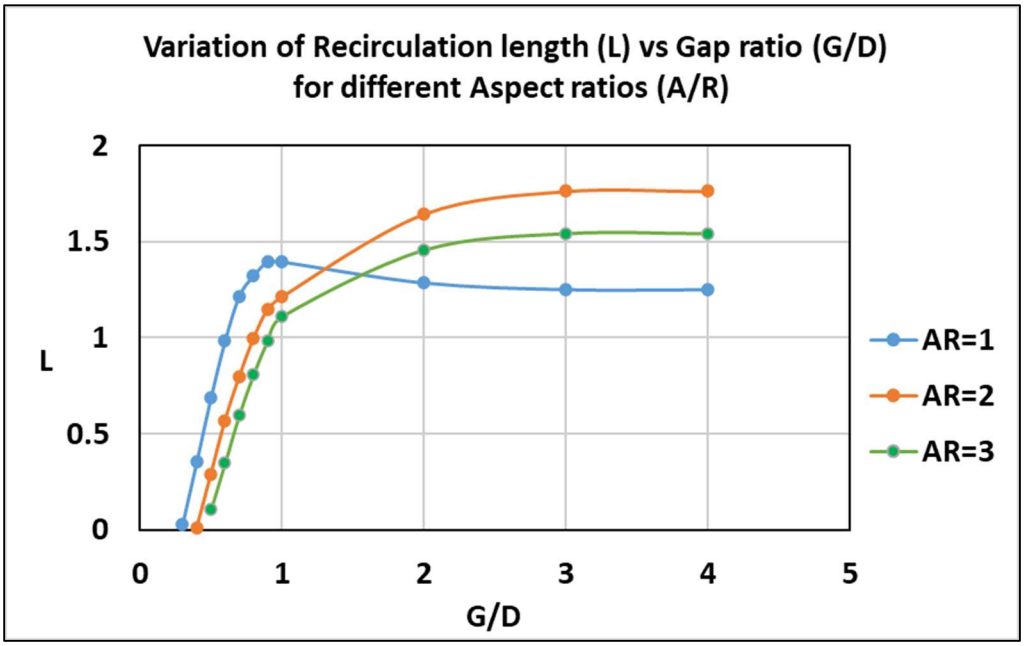


Fig. 32. Variation of Recirculation length L vs gap ratio for different aspect ratio of A/R = 1,2 & 3.

The above figure Fig. 18, shows variation of recirculation length for different aspect ratios with respect to variation in gap ratios. It can be seen that for higher gap ratios like 3 & 4 there is not much of difference between their respective recirculation lengths, whereas variation rises with decreasing the gap ratios from there onwards. For aspect ratio of 2 and 3 the length starts to decrease as we bring the rectangular bluff body closer to the stationary wall, whereas for aspect

ratio of 1 there is a slight jump in the value of recirculation length at gap ratio of 0.9 & 1 after which it decreases with its decreasing gap ratios, similar to its higher aspect ratio bodies.

4.7 Nusselt number

The Nusselt number (Nu) is the dimensionless number used in convective heat transfer analysis. It is used in heat transfer to compare convection with conduction at a surface. In simple terms, it tells how effectively a moving fluid transfers heat compared with a stagnant fluid layer. The Nusselt number (Nu) is the ratio of heat transfer by convection to the heat transfer by conduction within a fluid. The local Nusselt number (Nu) is defined in this study as,

$$\mathrm{Nu} = \frac{hL}{k},$$

Where, h represents the convective heat transfer coefficient, D represents the characteristic dimension & k being thermal conductivity.

4.7.1 Distribution of time average local Nusselt number along the surface of the rectangular cylinder for A/R=1,2 & 3.

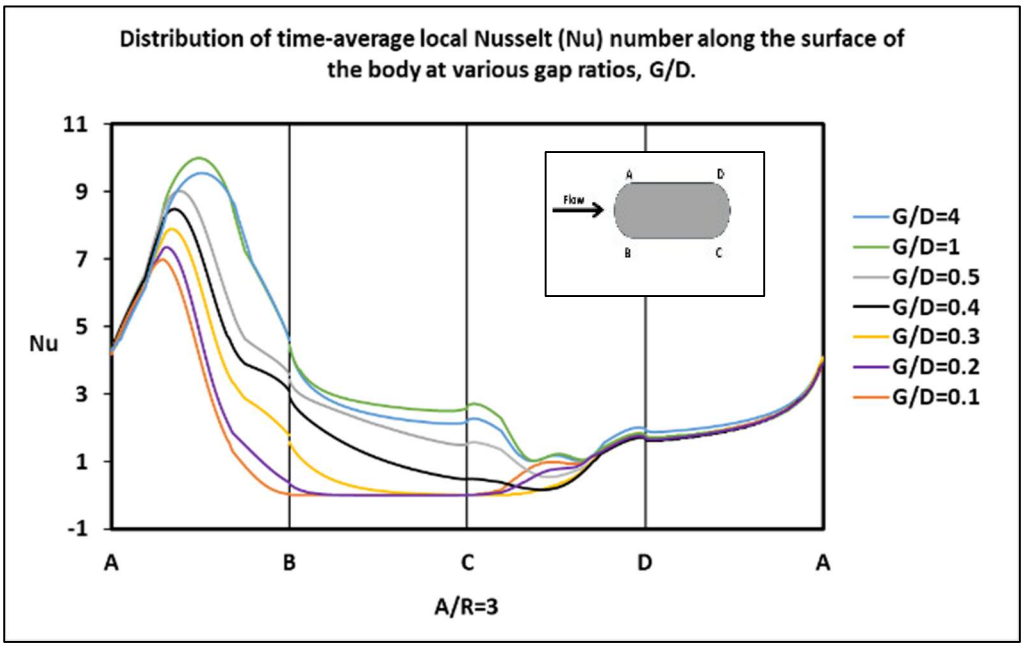


Fig. 33. Distribution of time averaged Nusselt number Nu on the surface of the body of aspect ratio A/R=3 near a stationary wall as a function of gap ratio, G/D.

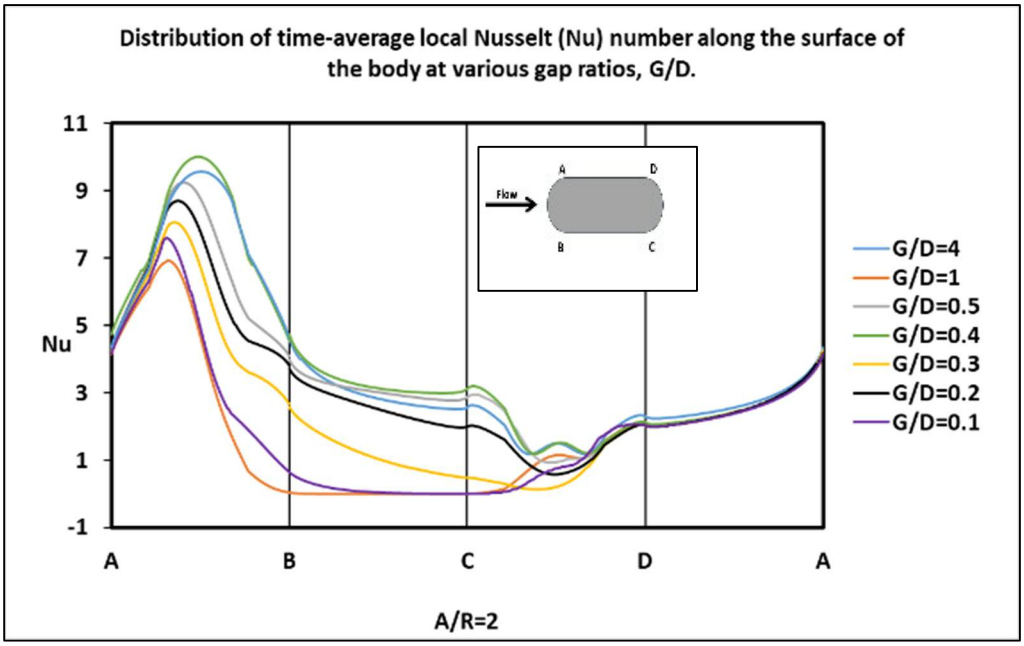


Fig. 34. Distribution of time averaged Nusselt number Nu on the surface of the body of aspect ratio A/R=2 near a stationary wall as a function of gap ratio, G/D.

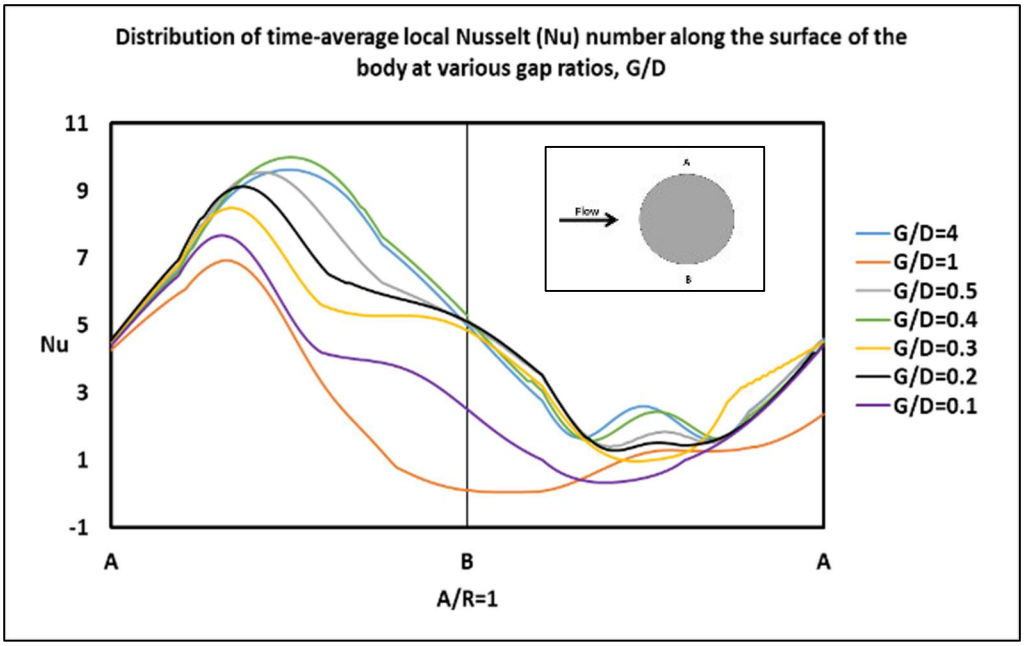


Fig. 35. Distribution of time averaged Nusselt number Nu on the surface of the body of aspect ratio A/R=1 near a stationary wall as a function of gap ratio, G/D.

Variation of Nusselt number (Nu) along the surface of the rectangular bluff body can be seen in the above figure Fig. 19, Fig.20 and Fig. 21 for A/R=3,2 & 1. The surface geometry of the bluff body is divided into four parts for A/R= 2 & 3 namely front,top,bottom and rear surfaces whereas for A/R = 1 is divided into two equal parts of front and rear surfaces.

Regardless of the A/R highest peak in the magnitude of Nusselt number (Nu) is seen to be present in the front surfaces as it is facing the flow. Variation of Nusselt number (Nu) with respect to gap ratio is more in front and bottom surfaces compared to rear and top surface where they converge together to a narrow range.

If we average the Nusselt number (Nu) for entire surface and plot it with respect to different gap ratios, it can be depicted as figure shown below:-

4.7.2 Average Nusselt number along the faces of rectangular cylinder for A/R=1,2 & 3.

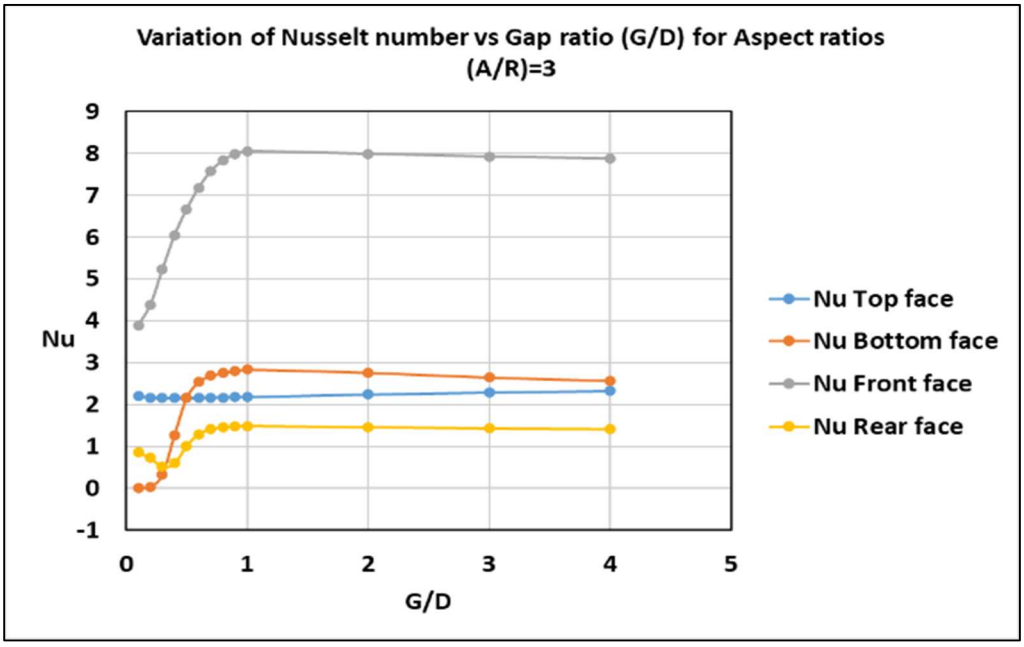


Fig. 36. Average Nusselt number Nu along the faces of rectangular cylinders for A/R=3 at different gap ratios G/D.

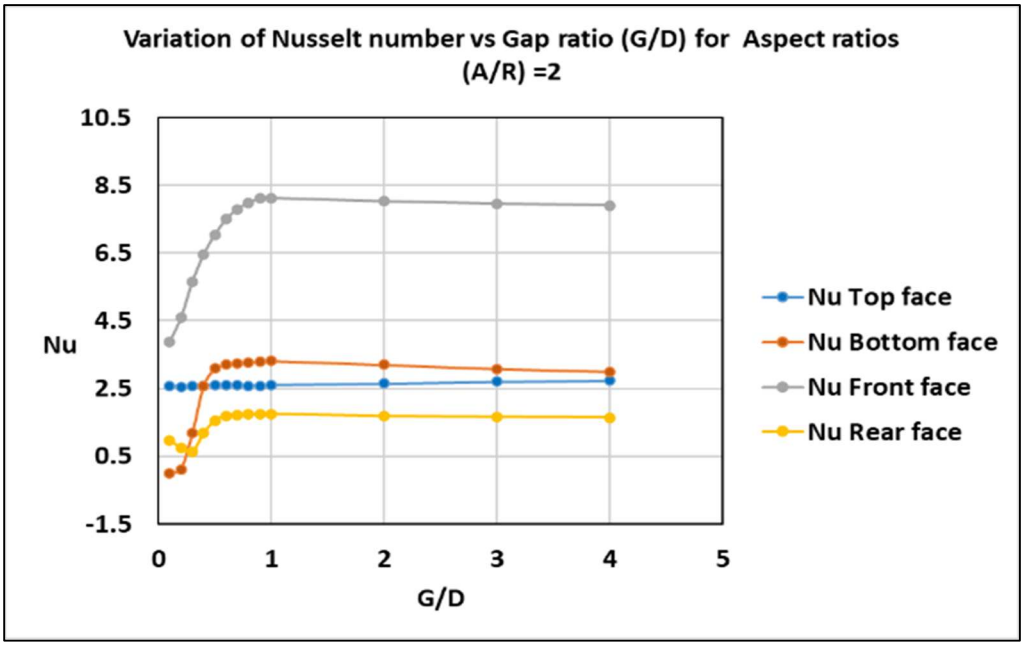


Fig. 37. Average Nusselt number Nu along the faces of rectangular cylinders for A/R=2 at different gap ratios G/D.

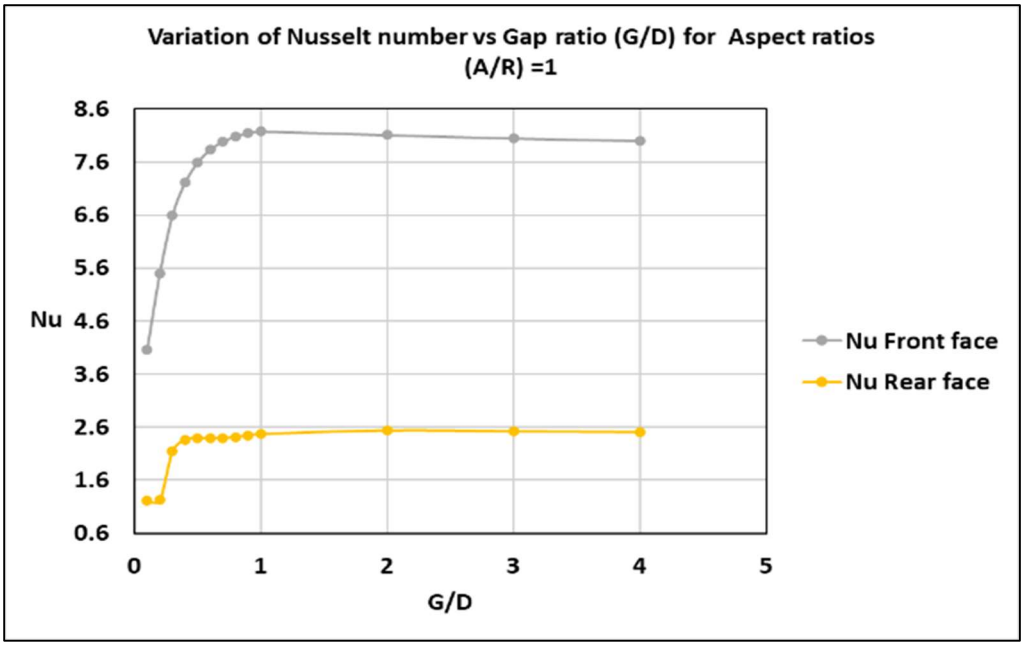


Fig. 38. Average Nusselt number Nu along the faces of rectangular cylinders for A/R=1 at different gap ratios G/D.

From the above figure Fig. 22,Fig. 23 and Fig. 24 it is evident that the front surface of the rectangular bluff bodies holds higher average Nusselt number (Nu) for an entire range of gap ratios compared to other surfaces of the body. A stable constant value of average Nusselt number (Nu) can be seen on the top surface throughout all gap ratios ,whereas for other surfaces the value is seen to dip for gap ratios lower than 1. Even though the overall average value of Nusselt number (Nu) for rear surface is lower compared to other surfaces, the bottom surface is seen to achieve lowest value for gap ratio of 0.2 & 0.1 .

4.7.3 Mean Nusselt number

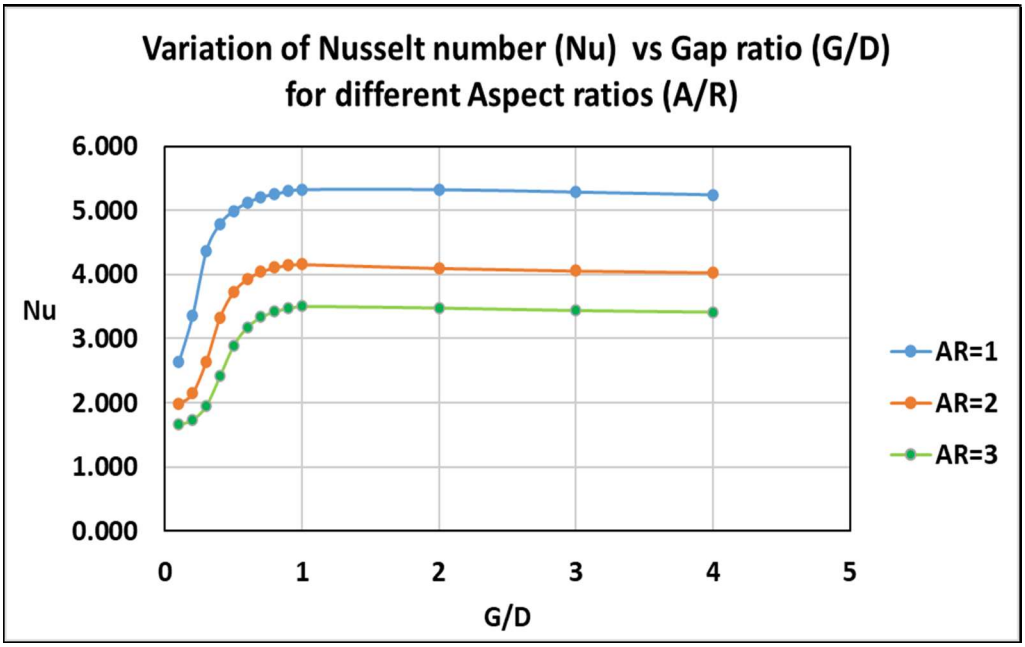


Fig. 39. Variation of mean Nusselt number Nu vs gap ratio for different aspect ratio of A/R = 1,2 & 3.

Above fig. Fig. 25 illustrates how the Nusselt number (Nu) varies with the Gap ratios for different aspect ratios of bluff bodies, with the Reynolds number (Re) set at 100. For the rectangular bluff body, the Nusselt number (Nu) remains relatively the same for gap ratios greater than 1. At a gap ratio of 1, the Nusselt number (Nu) is seen to be maximum for the respective aspect ratios i.e. about, and for the aspect ratios of 1,2 and 3 respectively . As we further decrease the gap ratio, a

steep decrease in Nusselt number (Nu) can be observed going as low as for aspect ratios of 2 & 3.Although not much of a difference in Nusselt number (Nu) can be seen in between different gap ratios for lower gap ratios. This pattern indicates that the rectangular bluff body is more sensitive to changes in the gap ratio when it is below 1 with very less influence of aspect ratio for the same range, but for higher gap ratios an observable difference can be identified with respect to aspect ratios.

Chapter 5

Summary and Conclusions

This study investigates the effects of aspect ratios A/R and gap ratios G/D on the flow around rectangular cylinder with rounded edges when placed in proximity to stationary wall at Re=100.

The results shared describes the effect on various flow parameters like Lift coefficient Cl, drag coefficient (Cd), Strouhal number (St), Nusselt number (Nu) of rectangular cylinder.

Simulation were carried out for gap ratios G/D ranging from 0.1 to 4 and three different aspect ratios i.e A/R=1,2&3 placed in a domain consisting of air flow with uniform velociity and stationary plane wall beside the body using SIMPLE algorithm. The key findings from the above study can be concluded as:-

1. With an increase in aspect ratio from A/R=1 to 3, flow is more stabilized around the body due to increase in streamwise length of the body as can be observed in vorticity contour figure.

2. The two row vortex shedding can be seen for higher gap ratio and with decreasing gap ratios the shedding also decreases due to influence of the plane wall. For aspect ratio A/R=1, the influence of plane wall on the vortex shedding of the body starts for gap ratio G/D=<0.7, whereas for aspect ratio A/R=2 the same occurs at gap ratio G/D=<2. Therefore, it can be said that the gap ratio at which the two row vortex diminishes moves to lower gap ratios G/D with decreasing aspect ratios.

3. The average drag coefficient (Cd) for higher aspect ratio body is lower compared to lower aspect ratio body. With decreasing gap ratios, the magnitude decreases slightly with very little variation until the gap ratio G/D=1. Further decrease in gap ratio G/D<1, a sudden drop is drag coefficent (Cd) is achieved. Unlike drag coefficent (Cd), for average lift coefficient (Cl) the higher aspect ratio body tends to have more lift coefficient (Cl) compared to lower aspect ratio. The nature of the magnitude for gap ratio 4>=G/D>=1, is similar to that of drag coefficient (Cd), with slight in increase in magnitude as aspect ratio

increases. With further decrease in gap ratio G/D<1, the lift coefficient (Cl) increases at a much higher rate than before. For the very low gap ratios like G/D=0.1,0.2, a sudden dip can be seen in the magnitude.

4. For the range of gap ratios 4>=G/D>=1,the average pressure coefficient (Cp) for top, front and rear surfaces does not have much fluctuation but for bottom surface there is an increase in magnitude with decreasing gap ratio. For G/D<=1, all surfaces show an increase in pressure coefficient (Cp) with bottom surface increasing at at much higher rate compared to other three surfaces followed by drop in magnitude for all four surfaces at lower gap ratios. For gap ratio ranging from 1<=G/D<=4, the strouhal number (St) is seen to increase, and starts to decrease if gap ratio is decreased further with least being at G/D=0.7 caused due to influence of stationary plane wall adjacent to the body.

5. Comparing between aspect ratios, higher aspect ratio of A/R=3 seem to posses lower average Nusselt number (Nu) compared to lower aspect ratio of A/R=1. For gap ratios ranging between 1<=G/D<=4, the average Nusselt number (Nu) has very little to no variation irrespective of the aspect ratio, only when the gap ratio starts to decrease below 1 , the magnitude of the Nusselt number (Nu) can be seen to decrease initially at slower rate and much higher rate as gap ratio decreases further. The average surface Nusselt number (Nu) for top surface of the body is almost constant with very low variation for the entire range of gap ratios. Similar nature can be seen for other surface only for limited range of gap ratios ranging from 1<=G/D<=4. When the gap ratio decreases below , a decrease in the magnitude of average nussselt number can be observed for the same mentioned three surfaces.

REFERENCES

[1] R. Wang et al., “Numerical study of the effects of aspect ratio and Reynolds number on the flow over a rectangular cylinder with rounded corners,” Ocean Eng., vol. 297, p. 117115, Apr. 2024, doi: 10.1016/j.oceaneng.2024.117115.

[2] J. Zhou, J. Ren, D. Li, P. Wang, and W. Bai, “Numerical investigation of flow field characteristics around semi-submerged rectangular cylinders with rounded corners,” Ocean Eng., vol. 299, p. 117441, May 2024, doi: 10.1016/j.oceaneng.2024.117441.

[3] S. Zhai and G. Xi, “The Effect of the Gap Ratio on the Flow and Heat Transfer over a Bluff Body in Near-Wall Conditions,” Fluid Dyn. Mater. Process., vol. 18, no. 1, pp. 109–130, 2021, doi: 10.32604/fdmp.2022.018186.

[4] H. Chalmers, X. Fang, and M. F. Tachie, “Gap ratio effects on the coherent structures surrounding a near-wall square cylinder,” Int. J. Heat Fluid Flow, vol. 100, p. 109114, Apr. 2023, doi: 10.1016/j.ijheatfluidflow.2023.109114.

[5] H. Helmizar et al., “Flow Characteristics Around Circular and Rectangular Bluff Bodies Near a Wall at Varying Gap Ratios,” J. Adv. Res. Fluid Mech. Therm. Sci., vol. 133, no. 2, pp. 238–254, Jul. 2025, doi: 10.37934/arfmts.133.2.238254.

[6] “Effect of gap flow on the shallow wake of a sharp-edged bluff body—Coherent structures,” ResearchGate. Accessed: May 21, 2026. [Online]. Available: https://www.researchgate.net/publication/325865930_Effect_of_gap_flow_on_the_shallow_wake_of_a_sharp-edged_bluff_body-Coherent_structures

[7] “Two-Dimensional Vortex Shedding from a Circular Cylinder near a Moving Wall,” ResearchGate. Accessed: May 21, 2026. [Online]. Available: https://www.researchgate.net/publication/271770658_Two-Dimensional_Vortex_Shedding_from_a_Circular_Cylinder_near_a_Moving_Wall

[8] E. Lamballais, J. Silvestrini, and S. Laizet, “Direct numerical simulation of a separation bubble on a rounded finite-width leading edge,” Int. J. Heat Fluid Flow, vol. 29, no. 3, pp. 612–625, Jun. 2008, doi: 10.1016/j.ijheatfluidflow.2008.03.006.

[9] T. Abdelhamid, Md. M. Alam, and Md. Islam, “Heat transfer and flow around cylinder: Effect of corner radius and Reynolds number,” Int. J. Heat Mass Transf., vol. 171, p. 121105, Jun. 2021, doi: 10.1016/j.ijheatmasstransfer.2021.121105.

[10] S. Dhinakaran, “Heat transport from a bluff body near a moving wall at Re=100,” Int. J. Heat Mass Transf., vol. 54, no. 25–26, pp. 5444–5458, Dec. 2011, doi: 10.1016/j.ijheatmasstransfer.2011.07.046.

[11] “Flow Past a Square Cylinder Near a Wall in the Absence of Wall Boundary-Layer,” ResearchGate. Accessed: May 18, 2026. [Online]. Available: https://www.researchgate.net/publication/331159822_Flow_Past_a_Square_Cylinder_Near_a_Wall_in_the_Absence_of_Wall_Boundary-Layer

[12] B. G. Dehkordi, H. S. Moghaddam, and H. H. Jafari, “Numerical Simulation of Flow Over Two Circular Cylinders in Tandem Arrangement,” J. Hydrodyn., vol. 23, no. 1, pp. 114–126, Feb. 2011, doi: 10.1016/S1001-6058(10)60095-9.

[13] S. Kang, “Characteristics of flow over two circular cylinders in a side-by-side arrangement at low Reynolds numbers,” Phys. Fluids, vol. 15, no. 9, pp. 2486–2498, Sep. 2003, doi: 10.1063/1.1596412.

[14] K. Liu, D. Ma, D. Sun, and X. Yin, “Wake Patterns of Flow Past a Pair of Circular Cylinders in Side-by-Side Arrangements at Low Reynolds Numbers,” J. Hydrodyn., vol. 19, no. 6, pp. 690–697, Dec. 2007, doi: 10.1016/S1001-6058(08)60005-0.

[15] K. Lee and K.-S. Yang, “Flow patterns past two circular cylinders in proximity,” Comput. Fluids, vol. 38, no. 4, pp. 778–788, Apr. 2009, doi: 10.1016/j.compfluid.2008.07.005.

[16] J. Park, K. Kwon, and H. Choi, “Numerical solutions of flow past a circular cylinder at Reynolds numbers up to 160,” KSME Int. J., vol. 12, no. 6, pp. 1200–1205, Nov. 1998, doi: 10.1007/BF02942594.